# Use of Dowel Bars at Longitudinal Construction Joints

Soojun Ha, Luis Cobos, Seong Cheol Choi,
Jungheum Yeon, Byounghooi Cho,
Moon C. Won

**NOTICE**

The United States Government and the State of Texas do not endorse products or manufacturers. Trade or manufacturers' names appear herein solely because they are considered essential to the object of this report

| 1. Report No. FHWA/TX -11-0-6190-1 | 2. Government Accession No.: | 3. Recipient's Catalog No.: |
|---|---|---|
| 4. Title and Subtitle: Use of Dowel Bars at Longitudinal Construction Joints | | 5. Report Date: August 2011 |
| | | 6. Performing Organization Code: |
| 7. Author(s): Soojun Ha, Luis Cobos, Seongcheol Choi, Jungheum Yeon, Byounghooi Cho, Moon C. Won | | 8. Performing Organization Report No. 0-6190-1 |
| 9. Performing Organization Name and Address: Texas Tech University College of Engineering Box 41023 Lubbock, Texas 79409-1023 | | 10. Work Unit No. (TRAIS): |
| | | 11. Contract or Grant No. : Project 0-6190 |
| 12. Sponsoring Agency Name and Address Texas Department of Transportation Research and Technology Implementation Office P. O. Box 5080 Austin, TX 78763-5080 | | 13. Type of Report and Period Cover: Technical Report 09/2008 – 08/2010 |
| | | 14. Sponsoring Agency Code: |

16. Abstract: The primary objective of this research project was to develop rational guidelines on the use of dowel bars in longitudinal construction joints (LCJs) for better-performing concrete pavements without potential longitudinal cracking problems. To thoroughly investigate the behavior of tied and/or doweled concrete pavements, field testing was conducted in several new continuously reinforced concrete pavement (CRCP) construction projects in Texas. Concrete strain gages, concrete displacement gages, and steel strain gages were installed in each test section. To achieve the primary objective of this study in a more effective way, theoretical analysis was performed along with field experimentation. It was found from field experimentation that subgrade drag theory (SGDT) – currently used for tie bar design – is not adequate to accurately analyze the behavior of concrete pavements. Accordingly, an improved numerical model based on plane strain theory was developed to analyze a concrete pavement with tie bars at LCJs. To verify the validity of the numerical model, the analysis results were compared with the field data – transverse displacements across the LCJs, concrete stresses, and tie bar stresses. The comparison indicated a good correlation when both frictional restraint and curling effects were included in the analysis. The influences of multiple lane ties and pavement geometries on the stresses in concrete and tie bars were investigated through parametric studies using the numerical model. Although the stresses in tie bars and concrete increase as more lanes are tied together, the growth slows due to bond slip at the interface between tie bars and concrete. This means that the dowel bar placement instead of tie bars could reduce concrete stresses if it applies to wide pavements, while it could result in lane separation problems. On the other hand, concrete stresses do not increase any further if four or more lanes are tied together, and concrete stresses may not be high enough to cause longitudinal cracking. There are many miles of CRCP in Texas where more than four lanes and inside and outside concrete shoulders are tied together, with no longitudinal cracking. Accordingly, it is recommended from the findings in this study not to use dowel LCJs, as is the current practice.

| 17. Key Words: Tie bars, dowels, longitudinal cracking, lane separation, number of lanes | | 18. Distribution Statement No restrictions. This document is available to the public through the National Technical Information Service, Springfield, VA 22161, www.ntis.gov | |
|---|---|---|---|
| 19. Security Classif. (of this report) Unclassified | | 20. Security Classif. (of this page Unclassified | 21. No. of Pages 92 | 22. Price |

# USE OF DOWEL BARS AT LONGITUDINAL CONSTRUCTION JOINTS

by

**Soonjun Ha**

**Luis Cobos**

**Seongcheol Choi**

**Jungheum Yeon**

**Byounghooi Cho**

**Moon C. Won**

Texas Tech University

Project Report 0-6190-1

Project Number 0-6190

Performed in Cooperation with the

Texas Department of Transportation

and the

Federal Highway Administration

Center for Multidisciplinary Research in Transportation

Department of Civil and Environmental Engineering

Texas Tech University

Box 41023

Lubbock, TX 79409-1023

# Acknowledgments

# Products

This report contains P1 "Guidelines for the construction practices to minimize longitudinal cracking" in Appendix A.

**AUTHOR'S DISCLAIMER**

The contents of this report reflect the views of the authors who are responsible for the facts and the accuracy of the data presented herein. The contents do not necessarily reflect the official view of policies of the Texas Department of Transportation or the Federal Highway Administration. This report does not constitute a standard, specification, or regulation.

**PATENT DISCLAIMER**

There was no invention or discovery conceived or first actually reduced to practice in the course of or under this contract, including any art, method, process, machine, manufacture, design or composition of matter, or any new useful improvement thereof, or any variety of plant which is or may be patentable under the patent laws of the United States of America or any foreign country.

**ENGINEERING DISCLAIMER**

Not intended for construction, bidding, or permit purposes.

**TRADE NAMES AND MANUFACTURERS' NAMES**

The United States Government and the State of Texas do not endorse products or manufacturers. Trade or manufacturers' names appear herein solely because they are considered essential to the object of this report.

# Table of Contents

# List of Tables

# List of Figures

ix

# CHAPTER 1 INTRODUCTION

Tie bars have been used at longitudinal construction joints (LCJs) to keep the lanes from separating, and to a lesser extent, to provide enhanced load transfer efficiency between lanes or between an outside or inside lane and tied shoulder. In contrast, dowel bars traditionally have been used almost exclusively at transverse contraction joints in jointed plain concrete pavement (JCP) to provide load transfer from one slab to the next.

Because the actions of tie bars and dowels are quite different, design methods for those bars are also vastly different. Currently, tie bars are designed based on subgrade drag theory (SGDT) which was developed several decades ago, while the design of dowels is primarily based on the work by Timoshenko, expanded later by Friberg and Bradbury. One of the key differences between the two design methods is that tie bar design is to address stresses due to temperature variations, while dowel bar design is based on limiting bearing stresses in concrete near dowels due to wheel loading applications.

According to SGDT, stresses in tie bars are directly proportional to the width of the slabs. As traffic has increased over the years, more lanes have been used that were tied together to prevent lane separations. The increased number of slabs tied together raised concerns regarding the potential for increased concrete stresses and resulting longitudinal cracks. To reduce the potential for longitudinal cracking, some state highway agencies started using dowels in LCJs, rather than tie bars. The concern described is valid in that, according to SGDT, the wider the pavement, the greater the stresses in tie bars and concrete. It is true that longitudinal cracks do occur, and once they do, there are no cost-effective and efficient repair methods. Field evaluations of a number of longitudinal cracks indicate they are primarily caused by insufficient saw-cut depth and/or late saw-cut at longitudinal warping joints (LWJs). Excessive built-in curling also appears to play a role in longitudinal crack development. These cracks were often observed in CRCP with only few lanes tied together. This indicates that the cracks were not necessarily due to tying too many lanes together. At the same time, there are CRCP sections where more than 7 lanes were tied together, but with no longitudinal cracking problems. In other words, SGDT might not be applicable for tie bar and transverse steel design. Research findings in TxDOT research project 0-5444, indicated that SGDT is not applicable to PCC pavement with relatively thick slabs. This is due to the fact that thicker slabs experience larger temperature variations through the slab depth than do thinner slabs. The larger temperature variations through slab depth cause curling of the slabs, and violate the very assumption made in SGDT, which is that slabs move one-dimensionally and a full contact is maintained at the interface between the slab and the subbase, making subbase friction a major force in the system.

1

The Houston District of the Texas Department of Transportation (TxDOT) has used dowels in LCJs in several projects. The sole purpose of the use of dowels in LCJs was to reduce the amount of transverse steel. According to TxDOT's Design Standards, CRCP(1)-03 and CRCP(2)-03, the spacing of transverse steel depends on the widths of the lanes tied together. In TxDOT, transverse steel design is also based on SGDT, and this is a natural result. For example, if the distance from a free edge to the other free edge is over 108-ft for 12-in and 13-in CRCP, the spacing for transverse steel is 1 ft. This is a large amount of steel required, increasing the initial cost of CRCP. Also, too much steel (longitudinal and transverse) at one plane might create a weak plane, potentially increasing the probability of horizontal cracking.

Based on the research findings from TxDOT research study 0-5444 in 2009, TxDOT revised its statewide CRCP standards for tie bars and transverse steel. In the new CRCP(1)-09 and CRCP(2)-09, tie bar and transverse bar spacing is not a function of the widths of lanes tied together. In the new standards, the spacing for transverse steel is 4-ft and that for tie bars is 2-ft. The spacing of 4-ft for transverse steel is based on the finding from 0-5444 that the stress in transverse steel is quite small, and as long as longitudinal cracks are prevented by good joint sawing practices, there is no need for too much transverse steel except for the support for the longitudinal steel. On the other hand, field evaluations show that tie bars play an important role in load transfer efficiency (LTE), and effective LTE and LCJ and LWJ will provide better performance of CRCP.

**Scope of the Report**

This research project was a joint project between Texas Tech University (TTU) and The University of Texas at Austin (UT). Research teams from both universities worked together in all aspects of this project.

Chapter 2 presents field evaluations conducted to measure stresses in concrete and tie bars.

Chapter 3 discusses development and verification of numerical model with field data.

Chapter 4 presents the findings of numerical parametric study on tie bar design factors.

Chapter 5 presents conclusions and recommendations.

0-6190-1

# CHAPTER 2 FIELD EVALUATION OF STRESSES IN CONCRETE AND TIE BARS

Field testing was conducted in two locations – one in Belton, Waco District and the other in Lubbock, Lubbock District – to evaluate the potential for longitudinal cracking in response to the increase in concrete stresses that might result from tying a number of lanes together. Evaluation of cracking potential in concrete requires accurate estimation of concrete stresses. Because the longitudinal cracking that could result from tying too many lanes together is due to environmental loading, concrete stresses due to environmental loading need to be accurately evaluated. In addition, field testing was conducted to evaluate steel strains. Because the concrete stresses in the transverse direction will depend on the restraint provided by tie bars and dowel bars in addition to other factors, it is quite important to obtain stress information in tie bars and dowel bars in order to fully understand the stress field near longitudinal construction joints (LCJs). These stresses along with environmental condition, material properties, and pavement geometry information will be used to calibrate the model developed in Chapter 3.

## 2.1 Field Testing Program

### 2.1.1 Measurement of concrete stresses

**2.1.1.1 Test section in Waco District:** A new continuously reinforced concrete pavement (CRCP) construction project located on Interstate Highway 35 south bound in Belton, the Waco District of the Texas Department of Transportation (TxDOT) was select to measure concrete stresses. Concrete was poured at 6:30 a.m., October 28th, 2009. The test slab consists of a new 14 inch-thick CRCP over a 4 inch-thick asphalt stabilized base. As shown in Figure 2.1, two layers of longitudinal steel were placed at depths of 4⅜ and 8⅜ in., with a spacing of 9½ in. The new slab was 22 ft wide and tied with the existing lane through two layers of tie bar. The existing lane consists of three lanes, which have the widths of 8, 16, and 12 ft, respectively. The two layers of tie bar were placed at depths of 5⅛ and 9⅛ in. along with transverse steels. Each layer of tie bar has a spacing of 3 ft. The longitudinal and transverse steels and tie bars have a diameter of ¾ in. (#6 steel).

*Figure 2.1: Overview of test section*

Gages were installed in two different test sections: tie bars were placed as designed originally in one test section and dowel bars were placed instead of tie bars in the other section as shown in Figure 2.2. Given environmental loading, the behavior of the two sections was expected to be different from each other because the existing and new lanes of CRCP were connected by different types of bars at LCJ.



*Figure 2.2: Tied and doweled sections*

4
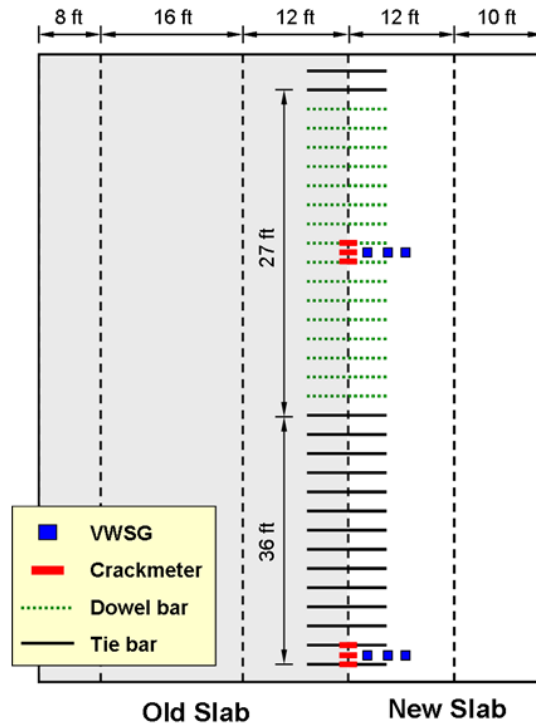
*Figure 2.3: Field instrumentation*

Figure 2.3 shows two types of gages installed in each test section: vibrating wire strain gages (VWSG) and crackmeters. To estimate the risk of longitudinal cracking in CRCP, three VWSGs were installed in the transverse direction at a depth of 1 in. from the surface of CRCP, as shown in Figure 2.4. These VWSGs were placed at different distances of 1, 5, and 10 ft from the LCJ. The strain measured by VWSGs can be used to estimate strains and stresses in the transverse direction and consequently the risk of longitudinal cracking in CRCP.

5

(a) VWSG installed with a chair
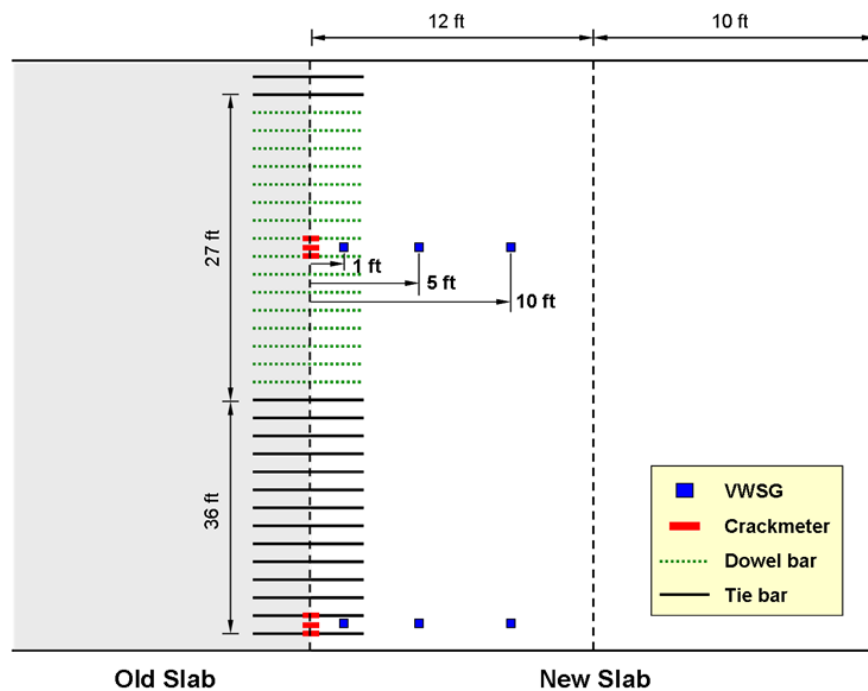


(b) Location of VWSGs

*Figure 2.4: VWSGs installed in the field*

As shown in Figure 2.5, crackmeters which can measure the displacement of CRCP were installed at the surface across the LCJ on Day 82 after concrete placement. Since upper and

6

lower tie bars (or dowel bars) were placed one after the other, three crackmeters were placed: the first one was located on the vertical extension of top layer of bars, the second one on that of the bottom layer of bars, and the third one in between. The displacement measured by each crackmeter was expected to be different from each other because the intensity of restraint would depend on the distance between the measured concrete element and the bars.



(a) Crackmeters installed at the surface across the LCJ in the tied section
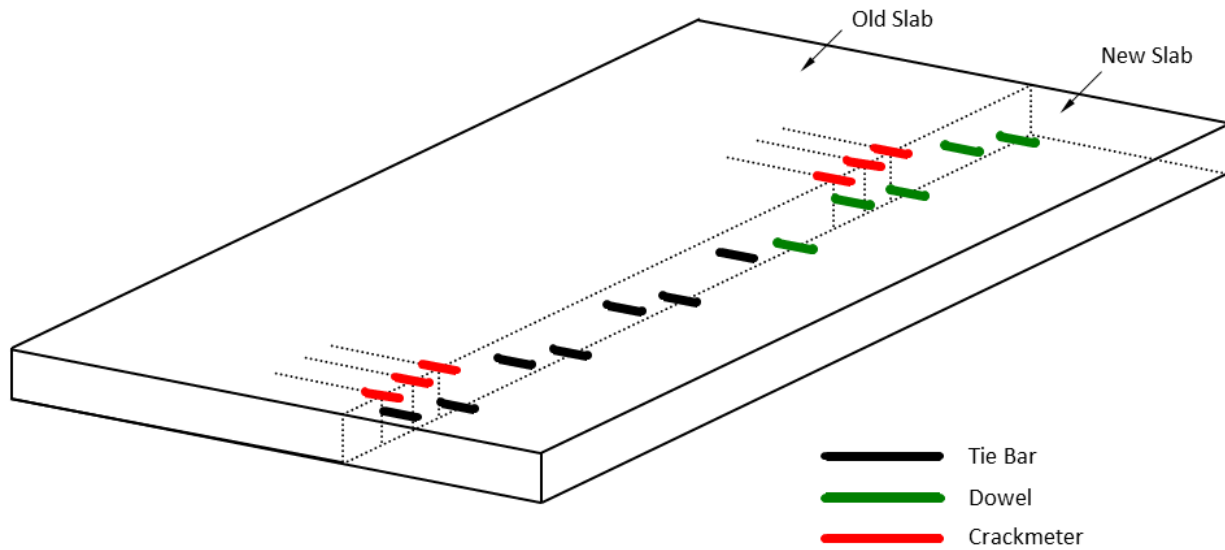


(b) Location of crackmeters

*Figure 2.5: Crackmeters installed in the field*

7

**2.1.1.2 Test section in Lubbock District:** A multilane CRCP section was constructed on Slide Avenue under the Marsha Freeway, Lubbock, Texas. Six lanes of two traffic directions are connected by a medium turning lane, and the width of every lane is 12 ft. 7 inch-thick concrete was placed on the asphalt stabilized subbase. The construction was divided into three stages, the sequence was north bound, south bound, and turning lane. The instrumentations were installed in the south bound construction, which was performed in two phases. Firstly, the concrete of the inside two lanes was placed at 4:20 p.m., October 22$^{nd}$, 2009, followed by the construction of the outside lane at 4:00 p.m., October 26$^{th}$, 2009.
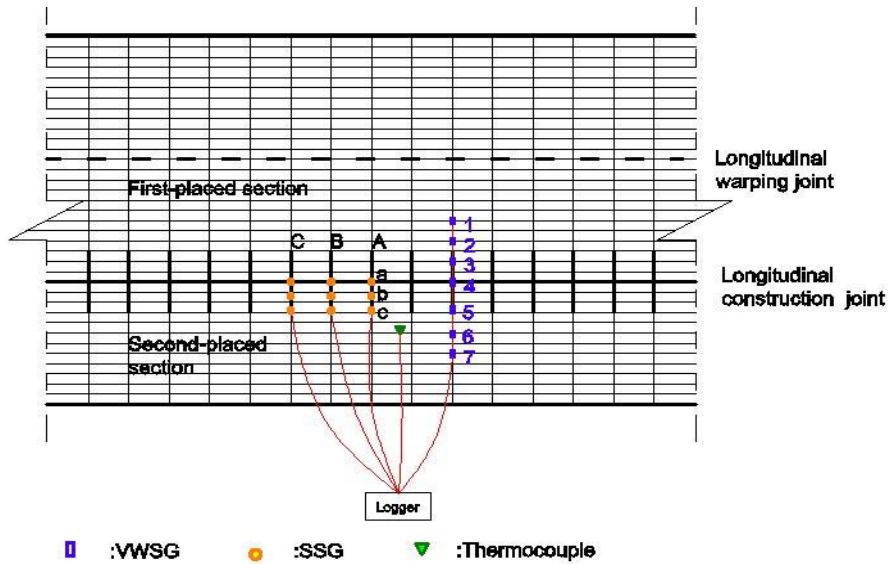


(a) Plan view
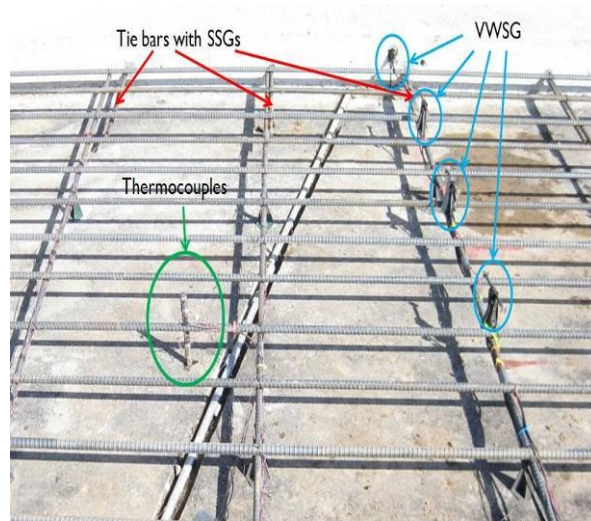


(b) Field layout of the instrumentations in the second-placed section

*Figure 2.6: Arrangement of the instrumentations*

Multi-pieces tie bars were installed at the LCJ to connect the two sections. Seven VWSGs were embedded transversely at 1 inch deep from the top surface of the pavement, one was arranged at the center of LCJ, and the other six were aligned at two sides of the joint symmetrically with the same spacing of 24 in. Nine steel strain gages (SSGs) were attached onto the top surface of the male piece of three tie bars abreast, located in the second-placed section. In order to measure the temperature variation of CRCP, a series of thermocouples were attached to a steel stick and embedded vertically in the second-placed concrete. The depths of the thermocouples to the top surface of the slab were 1.0, 2.5, 4.0, 5.5, and 6.0 in., respectively. All the instrumentations were connected to the Campbell Scientific logger CR1000 to download the data. The arrangements of the instruments are illustrated in Figure 2.6(a), and the field layout of the second-placed section was shown in Figure 2.6(b).

### 2.1.2 Measurement of tie bar stresses

To evaluate tie bar stresses due to environmental loading, field testing was conducted in two new CRCP construction projects in Texas, as shown in Figure 2.7: one in Rosenberg and the other in Fort Worth. In the Rosenberg section, the existing slab was 14 ft wide and a new 18 ft-wide slab with a thickness of 15 in. was placed with a LCJ in between. In Fort Worth, a new 12 ft-wide slab with a thickness of 8 in. was placed next to the existing 12 ft-wide slab. Tie bars were placed at mid-depth every 3 ft.
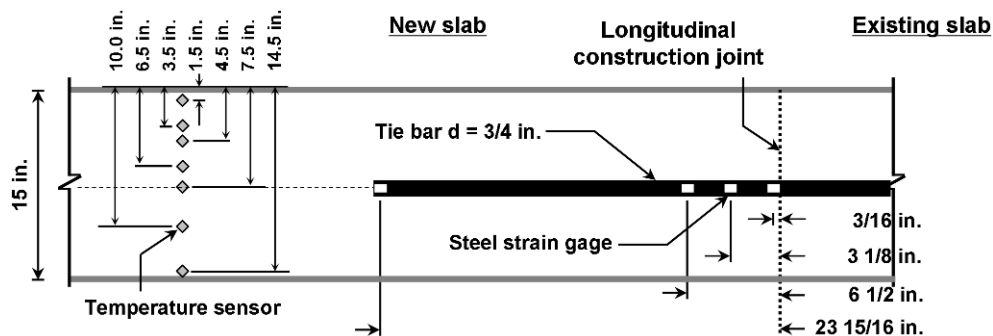


(a) Rosenberg section
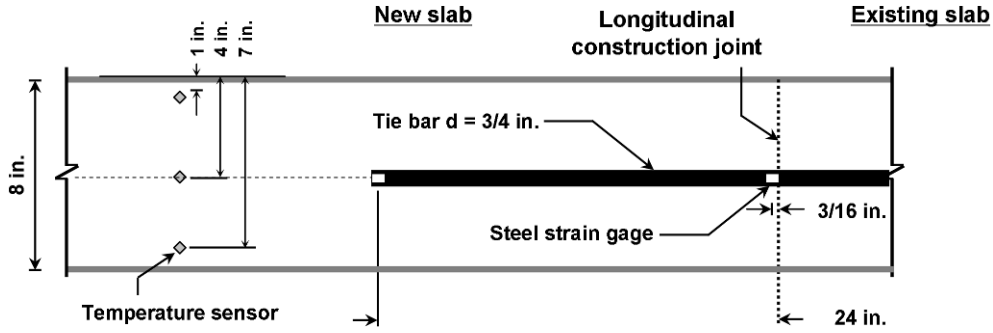
(b) Fort Worth section

*Figure 2.7: Test plan and details for gage installation*

Steel strain gages were installed at various locations of a tie bar as well as temperature sensors at a number of slab depths. The surface of a tie bar at planned gage installation locations was ground with a grinder and then polished with sandpaper to develop a flat and smooth surface for the steel strain gage installation. The accuracy of the steel strain measurements largely depends on the smoothness of the surface. In the Rosenberg section, to investigate the effect of tie bar spacing on tie bar stresses, two additional tie bars were inserted at 1-ft spacing between two adjacent tie bars with normal 3-ft tie bar spacing. To evaluate the effect of tie bar depth on tie bar stress, one tie bar was installed 5 in. from the surface of the slab, instead of the normal 7½-in. depth.

## 2.2 Method for Mechanistic Analysis of Measured Data

### 2.2.1 Constitutive relation of stress-strain in concrete

The method to calculate stress history from measured concrete strains is described. For the concrete element uniaxially loaded within service stress range, total strain $\varepsilon_i$ at time $t_i$ consists of stress-dependent strain $\varepsilon_i^\sigma$ and stress-independent strain $\varepsilon_i^0$ (Bažant, 1988). Stress-dependent strain which is produced by stresses is the sum of the instantaneous strain $\varepsilon_i^E$ – elastic if the stress is small – and creep strain $\varepsilon_i^C$. Stress-independent strain which is not related to stresses is the sum of thermal strain $\varepsilon_i^T$ and shrinkage $\varepsilon_i^{SH}$. Accordingly, total strain increment $\Delta\varepsilon_i$ during time step $\Delta t_i = t_i - t_{i-1}$ is expressed as follows:

$$\Delta\varepsilon_i = \Delta\varepsilon_i^E + \Delta\varepsilon_i^C + \Delta\varepsilon_i^T + \Delta\varepsilon_i^{SH} = \Delta\varepsilon_i^\sigma + \Delta\varepsilon_i^0 \tag{2.1}$$

10

where $\Delta\varepsilon_i^{\sigma} = \Delta\varepsilon_i^{E} + \Delta\varepsilon_i^{C}$ and $\Delta\varepsilon_i^{0} = \varepsilon_i^{T} + \Delta\varepsilon_i^{SH}$. The variation of stress arising from a prescribed strain history can be obtained through the principle of superposition as follows (Bažant, 1988):

$$\sigma(t) = \int_0^t R(t,t')[d\varepsilon(t') - d\varepsilon^0(t')] = \int_0^t R(t,t')\, d\varepsilon^{\sigma}(t') \tag{2.2}$$

where $\sigma(t)$ is stress history and $R(t,t')$ is the relaxation function which represents the stress at time $t$ caused by an increment of stress-dependent strain $d\varepsilon^{\sigma}(t')$ which was imposed at time $t_i$. The multi-axial generalization of stress-strain relation can be obtained with the assumption of isotropic material. Based on the hypothesis of linearity, Equation 2.2 is generalized as follows:

$$\boldsymbol{\sigma} = \int_0^t R(t,t')\,\mathbf{B}\,d(\boldsymbol{\varepsilon} - \boldsymbol{\varepsilon^0}) \tag{2.3}$$

$$\mathbf{B} = \frac{(1-v)}{(1+v)(1-2v)}\begin{bmatrix} 1 & v/(1-v) & v/(1-v) & 0 & 0 & 0 \\ & 1 & & 0 & 0 & 0 \\ & & 1 & 0 & 0 & 0 \\ & & & v^* & 0 & 0 \\ & & & & v^* & 0 \\ & & & & & v^* \end{bmatrix} \tag{2.4}$$

$$v^* = \frac{1-2v}{2(1-v)} \tag{2.5}$$

where $v$ is Poisson's ratio, $\boldsymbol{\sigma} = [\sigma_{11}\ \sigma_{22}\ \sigma_{33}\ \sigma_{12}\ \sigma_{23}\ \sigma_{31}]^{T}$, $\boldsymbol{\varepsilon} = [\varepsilon_{11}\ \varepsilon_{22}\ \varepsilon_{33}\ \varepsilon_{12}\ \varepsilon_{23}\ \varepsilon_{31}]^{T}$, and $\boldsymbol{\varepsilon^0} = [\varepsilon^0\ \varepsilon^0\ \varepsilon^0\ 0\ 0\ 0]^{T}$.

11
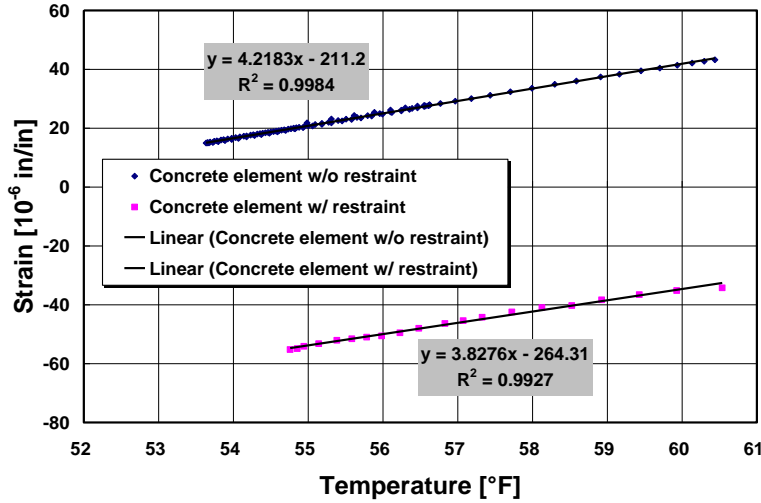
*Figure 2.8: Concrete strain vs. concrete temperature*

## 2.2.2 Degree of restraint

The mechanistic analysis was conducted with the data measured in Belton for the period when the crackmeter was being placed, i.e., afternoon of Day 82 to morning of Day 83, in Section 2.3.1.1. For a relatively short period, the contribution of creep and shrinkage to the development of stress is negligible and therefore Equation 2.1 is reduced as follows (Bažant, 1988):

$$\Delta \varepsilon_i = \Delta \varepsilon_i^{\mathrm{E}} + \Delta \varepsilon_i^{\mathrm{T}} \tag{2.6}$$

Figure 2.8 shows the rate of concrete strain caused by temperature changes which was measured for the period specified above. The concrete strain was measured in two different locations: one concrete element without restraint inside non-stress cylinder (NC) and the other concrete element at a distance of 1 ft from the LCJ which was restrained by tie bars. The slope of the linear regression line in Figure 2.8 is related to the degree of restraint on concrete volume changes. The degree of restraint is defined as follows (Nam et al., 2007):

$$R_i = 1 - \frac{\Delta \varepsilon_i}{\Delta \varepsilon_i^{\mathrm{f}}} = 1 - \frac{s_i \, \Delta T_i}{s_i^{\mathrm{f}} \, \Delta T_i} \tag{2.7}$$

where $R_i$ is the degree of restraint, $\Delta \varepsilon_i^{\mathrm{f}}$ is the change in strain of unrestrained concrete, $\Delta \varepsilon_i$ is

12

the change in strain of restrained concrete, and $s_i^f$ and $s_i$ are the slopes of linear regression line for unrestrained and restrained concrete [/$^o$F], respectively. Since $s_i^f$ means the coefficient of thermal expansion (CTE), Equation 2.7 can be expressed as follows (Kim and Won, 2008).

$$R_i = 1 - \frac{s_i}{\alpha_c} \qquad (2.8)$$

where $\alpha_c$ is CTE [/$^o$F]. The degree of restraint at a distance of 1 ft from the LCJ in the tie bar section was 9.2%, which means that only 9.2% of free movement was restrained in the concrete element. Higher degrees of restraint yield higher concrete stresses. For a given temperature variation $\Delta T_i$, the stress-dependent strain is expressed in terms of the degree of restraint as follows:

$$\Delta \varepsilon_i^E = \Delta \varepsilon_i - \Delta \varepsilon_i^T = -R_i \, \alpha_c \, \Delta T_i \qquad (2.9)$$

### 2.2.3 Stress state in CRCP

To accurately estimate the concrete stress caused by temperature changes, it is necessary to install three VWSGs in three dimensions, i.e., in longitudinal, transverse, and vertical directions. However, plane stress condition may exist in the concrete elements where strains were measured because of following reasons: (1) CRCP is very thin compared with the length and width; (2) the top of the slab is in stress-free condition in vertical direction; and (3) the concrete elements are not close to transverse cracks or the LCJ where free movement is restrained by bars. The vertical stress component is negligible with this assumption and Equation 2.3 can be written as follows:

$$\Delta \sigma_i^{tr} = \frac{E_c}{1-v^2} (\Delta \varepsilon_i^{E,tr} + v \Delta \varepsilon_i^{E,lo}) \qquad (2.10)$$

where $\Delta \sigma_i^{tr}$ is the change in transverse stress, $\Delta \varepsilon_i^{E,tr}$ is the change in elastic transverse strain, $\Delta \varepsilon_i^{E,lo}$ is the change in elastic longitudinal strain, and $E_c$ is the elastic modulus of concrete. Since CRCP has a great dimension in length, it can be assumed that the movement of CRCP is completely restrained in the longitudinal direction unless the concrete element is close to transverse cracks. Accordingly, Equation 2.10 can be rewritten as follows:

13

$$\Delta\sigma_i^{\mathrm{tr}} = -\frac{E_{\mathrm{c}}}{1-v^2}(R_i^{\mathrm{tr}} + v\,R_i^{\mathrm{lo}})\,\alpha_{\mathrm{c}}\,\Delta T_i = -\frac{E_{\mathrm{c}}}{1-v^2}(R_i^{\mathrm{tr}} + v)\,\alpha_{\mathrm{c}}\,\Delta T_i \qquad (2.11)$$

where $R_i^{\mathrm{tr}}$ and $R_i^{\mathrm{lo}}$ are the degrees of restraint in transverse and longitudinal directions, respectively. Equation 2.11 implies that the transverse concrete stress caused by temperature changes can be calculated from the degree of restraint measured by VWSG and known CTE.
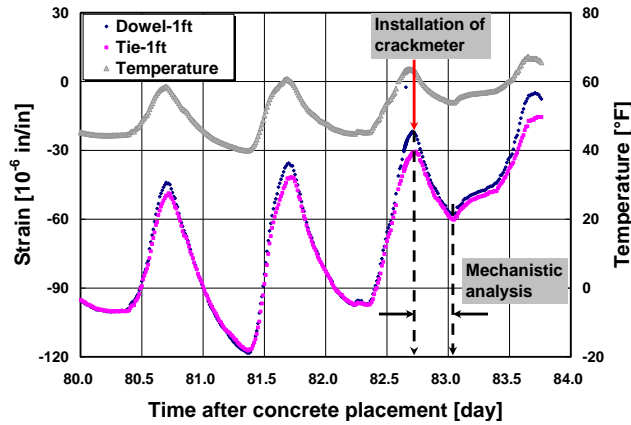


(a) At 1 ft from the LCJ
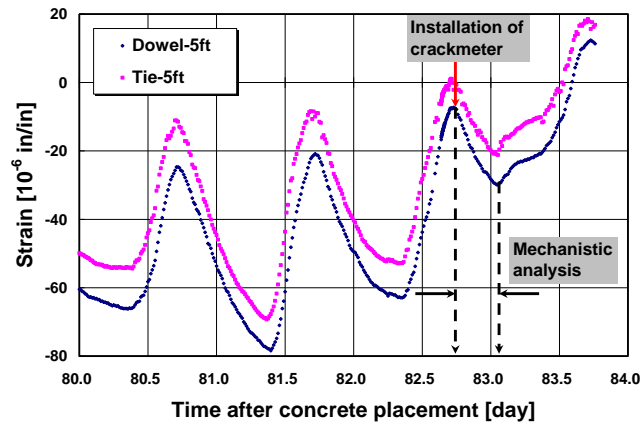


(b) At 5 ft from the LCJ
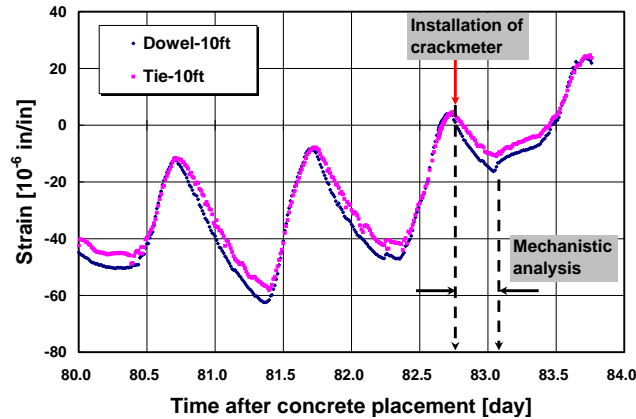
(c) At 10 ft from the LCJ

*Figure 2.9: Concrete strain measured in the tied and doweled sections*

## 2.3 Analysis of Measured Data

### 2.3.1 Concrete stresses

**2.3.1.1 Test section in Waco District:** Figure 2.9 shows the variation of concrete temperature and strain measured by VWSG in Belton. On the *x*-axis, the whole number denotes midnight of the day after concrete placement. For example, 81 indicates midnight on Day 81 after concrete placement. Even though the measurement began right after placing concrete, only a part of the data is shown because it represents the overall trend of variation in the entire monitoring period. As expected, the strain variation was similar to the temperature variation on the whole. The strain variation in the doweled section was greater than that in the tied section. This indicates that the movement of concrete was more restrained by tie bars than dowels, which agrees well with the current practice. However, the difference in restraints was not significant as much as was expected. The data measured during the period from afternoon of Day 82 to morning of Day 83 are used to estimate transverse concrete stresses. Figure 2.10 compares the strain variation at different distances from the LCJ. The movement of concrete was more restrained farther away from the LCJ.
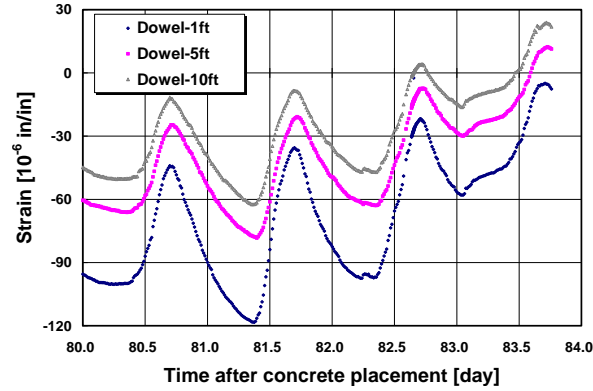
(a) Doweled section
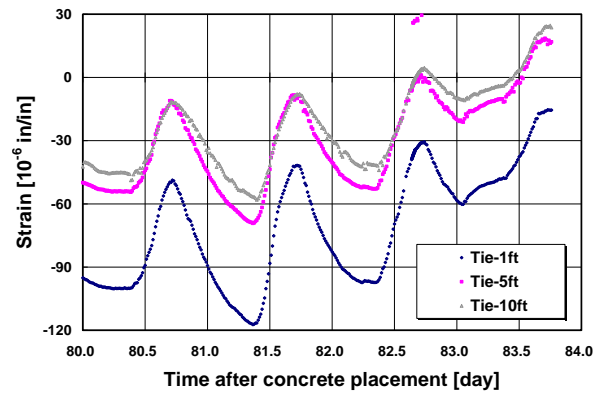


(b) Tied section

*Figure 2.10: Concrete temperature and strain measured at different distances from the LCJ*

Figure 2.11 shows the transverse displacement across the LCJ measured by crackmeters. As mentioned earlier, three crackmeters were installed at the surface with different vertical distances from tie bars (or dowel bars). The intensity of restraint on the concrete element was greater above the top layer of bars than above the bottom layer of bars. The movement of concrete at the LCJ was larger in the doweled section than in the tied section, which means that tie bars provide more restraints in the transverse direction.

0-6190-1
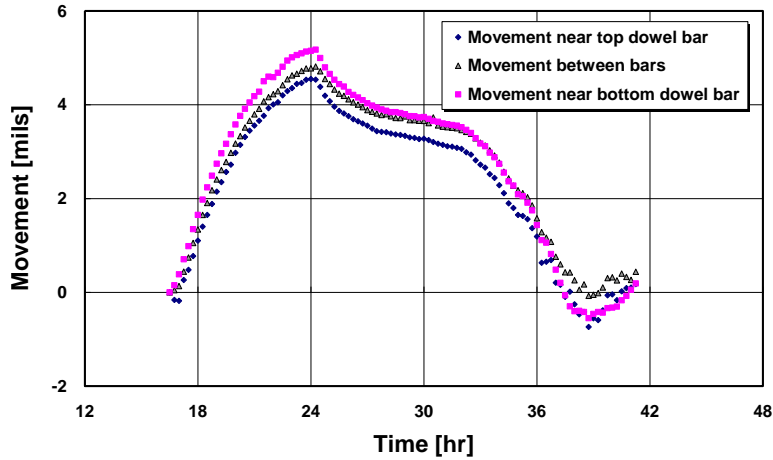
(a) Doweled section
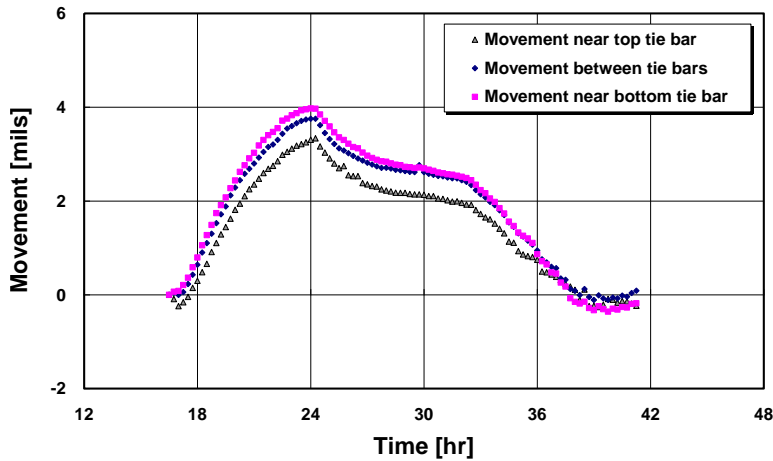


(b) Tied section

*Figure 2.11: Transverse displacement across the LCJ*

Figure 2.12 shows the NC installed in the field. This cylinder was to measure stress-independent concrete strain such as thermal strain and drying shrinkage (Kawaguchi and Nakane, 1996; Kim and Won, 2008). The design of NC is such that it isolates concrete inside it from the surrounding concrete and thus prevents the transfer of stress. Therefore, the VWSG in the NC measures the thermal strain of concrete under stress-free conditions, which is used to determine the CTE of concrete.

*Figure 2.12: Non-stress cylinder installed in the field*
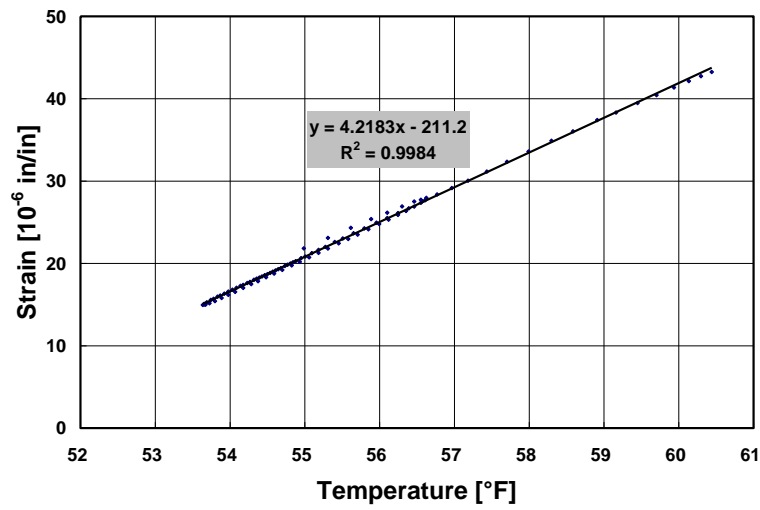


*Figure 2.13: Measured coefficient of thermal expansion of concrete*
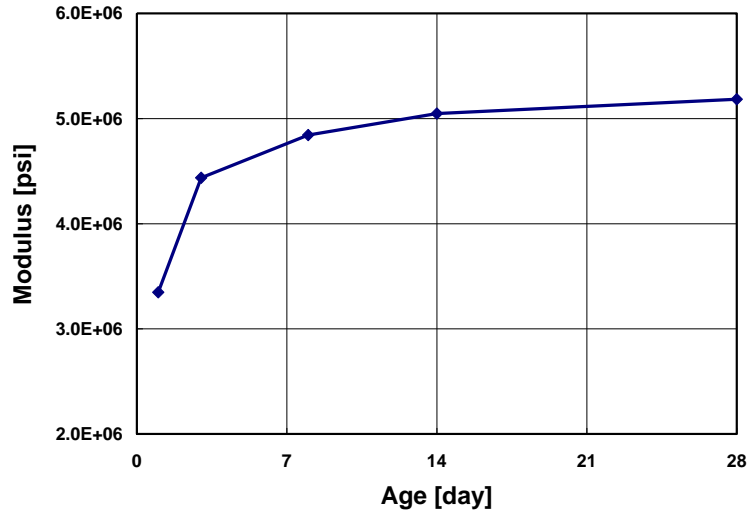
*Figure 2.14: Measured elastic modulus of concrete*

Figure 2.13 shows the rate of concrete strain caused by temperature changes measured in the NC. A good correlation was obtained between the variations of concrete strain and temperature. The CTE of concrete which corresponds to the slope of linear regression line was $4.22 \times 10^{-6}$ /°F. Figure 2.14 shows the measured elastic modulus of concrete. The elastic modulus of concrete on Day 28 was $5.18 \times 10^{6}$ psi. The concrete stress is calculated using Equation 2.11 with these values.

Figure 2.15(a) illustrates the distribution of concrete temperature along the depth axis in the tied section during the specified period (see Figure 2.9). The concrete temperature varied largely at the top of the slab. As shown in Figure 2.15(b), the temperature gradient was obtained from the distribution of concrete temperature, which will be used in the numerical analysis in Chapter 3. A second-order polynomial was used in the regression of the temperature gradient.
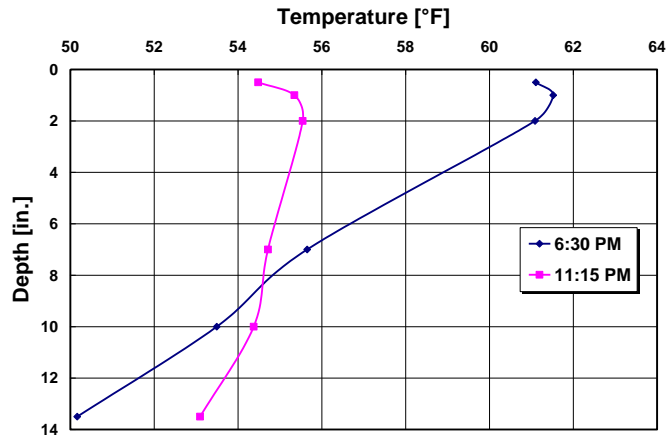
(a) Distribution along the depth axis
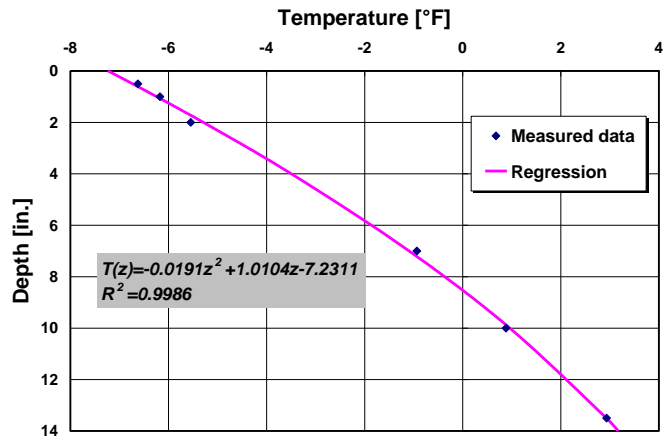


(b) Temperature gradient

*Figure 2.15: Concrete temperature measured in the tied section*
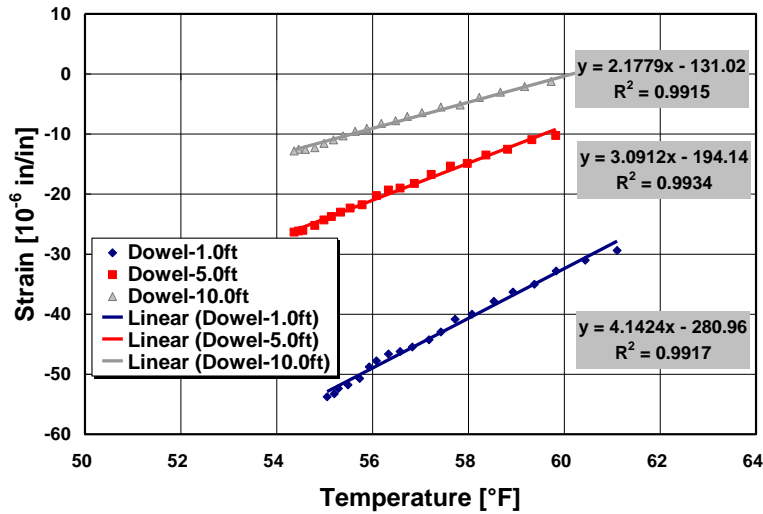
(a) Doweled section
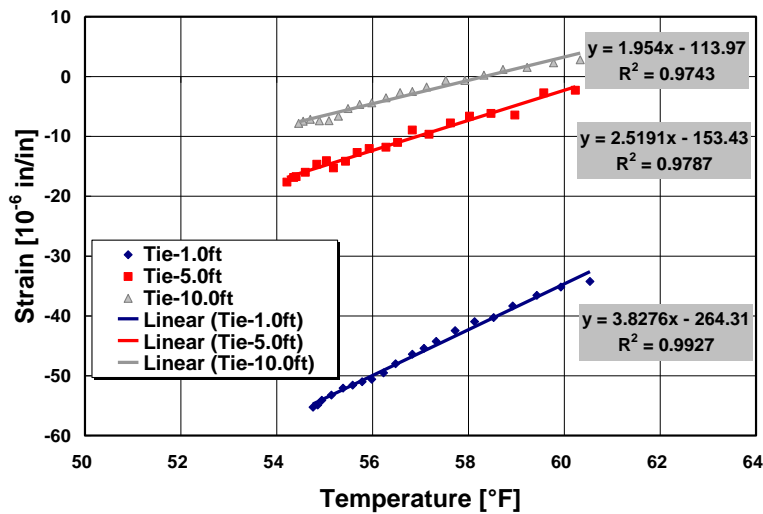


(b) Tied section

*Figure 2.16: Concrete strain vs. concrete temperature*

Figure 2.16 shows the rate of concrete strain caused by temperature changes at different distances from the LCJ. The slope of linear regression line decreases farther away from the LCJ. At the same distance from the LCJ, the slope is steeper in the doweled section than in the tied section, which means that tie bars provide more restraint on the concrete element. The degree of restraint at various distances from the LCJ in the two sections can be calculated using Equation

21

2.8 with the measured results in Figure 2.16.

For the temperature gradient in Figure 2.15, the transverse concrete stress was calculated using Equation 2.11 with the degree of restraint, the elastic modulus of concrete, and the CTE of concrete determined in Figure 2.16, 2.14, and 2.13, respectively. As shown in Figure 2.17, higher stresses developed farther away from the LCJ. Since tie bars provide more restraint on the concrete element, larger stresses developed in the tied section than in the doweled section.
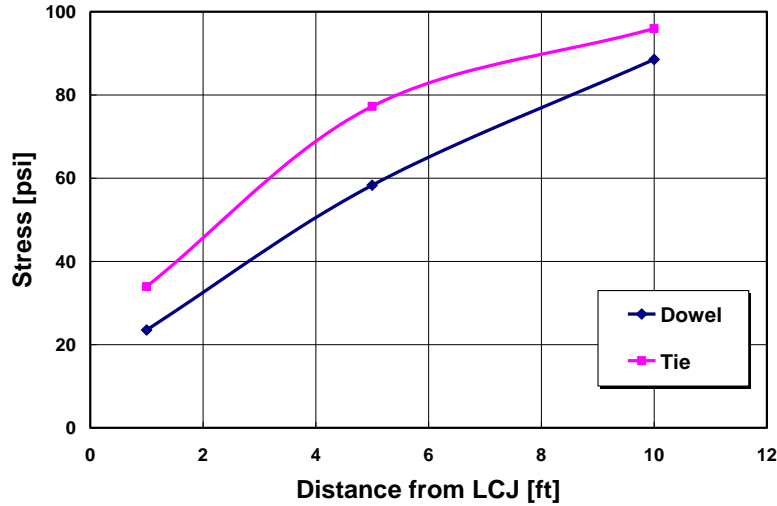


*Figure 2.17: Transverse concrete stress*
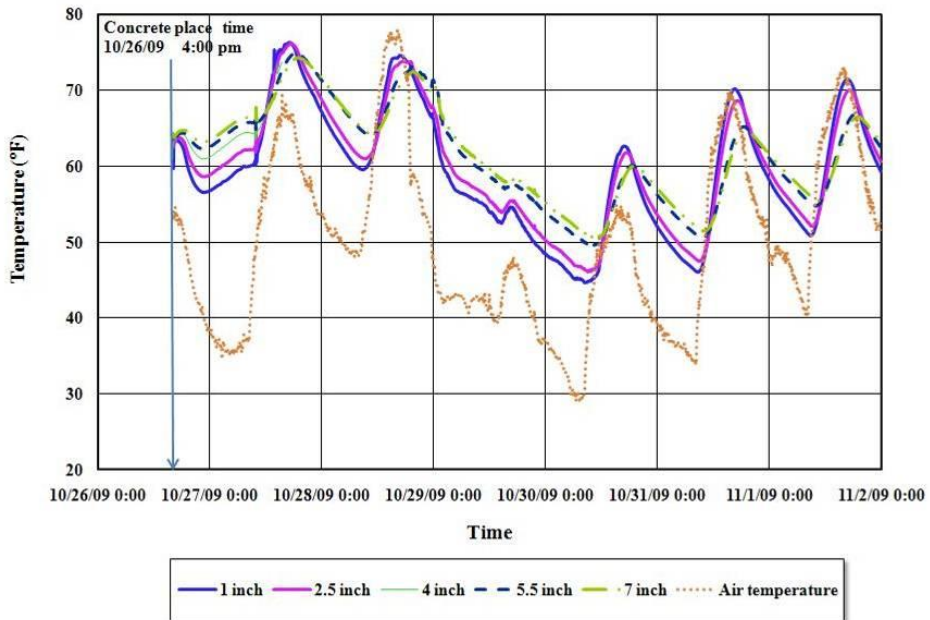


*Figure 2.18: Temperature of different depths varied with time through the first week*

**2.3.1.2 Test section in Lubbock District**

After the concrete placement, the behavior of the pavement had being monitored until January 4th, 2010, when the logger had to be removed from the site for the completion of this work. The results were analyzed and shown below.

*Temperature of the CRCP*

As is well known, the fluctuations in temperature produce expansion and contraction movements in concrete pavements, which lead to the development of stresses and possibly cracking, which may significantly affect the pavements early-age and long-term performance (McCullough and Rasmussen, 1998). On the other hand, it has been reported that the initial thermal gradient at setting (built-in curling) plays a major role in the long-term performance of jointed concrete pavement (Yu et al., 1998). During the hydration of concrete under field conditions, the concrete temperature development is determined by the balance between heat generation from the cementitious materials and heat exchange with the structure and its surroundings.
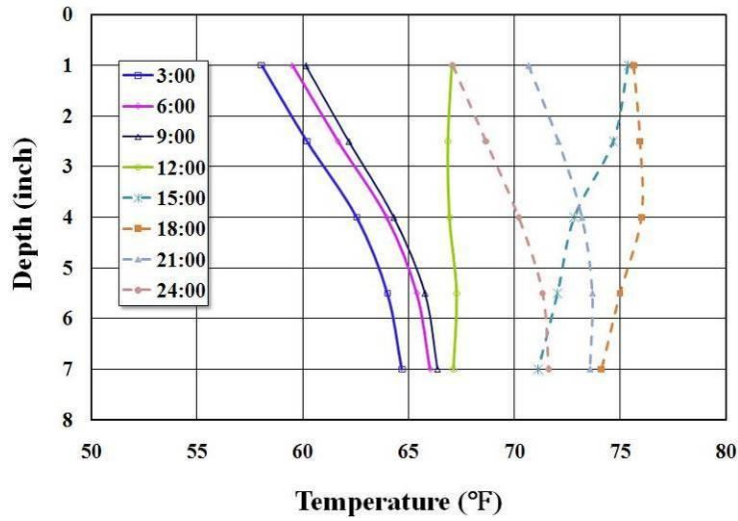
(a) October 27th, 2009
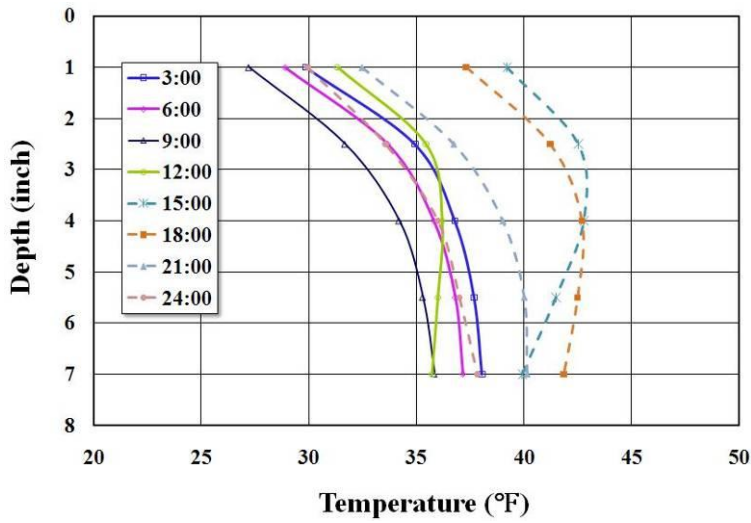


(b) December 3rd, 2009

*Figure 2.19: Temperature distribution along the depth*

The temperatures of the CRCP of the first week are illustrated in Figure 2.18, during the period of rapid cement hydrating, although the air temperature decreased evidently, the temperatures of the concrete increased mostly until it arrived at the highest value next afternoon. With the slowing down of the hydration, the concrete temperatures cycled as a similar trend of the air

24

temperature. On the other hand, the temperatures at different depths of the concrete slab changed differently, the nearer to the surface of the slab, the faster and more of the changes.

As discussed before, the effects of environmental factors on the concrete differed with depth, and induced the temperature gradient along the depth of the slab. The temperature distributions along the depth of the slab at two ages are shown in Figure 2.19, one is of three days and the other one is of 40 days when the lowest air temperature occurred. Both of them show a character of nonlinear distribution. The temperature gradient alternated between positive and negative in the cool weather (Figure 2.19(a)), but negative temperature gradient was behaved in Figure 2.19(b). With the variation of the temperature gradient, the concrete had the potential to expand or contract and the slab would curl up or down, but there were factors restrained the movement to some extent. The restrained factors include the reinforcement steel, tie bars between different sections along construction joint, and the supporting layers under the slab. Even though the movement of the concrete is restrained, the slab still moves.

*Strain of the slab and the longitudinal construction joint*

The VWSGs embedded in the first-placed section were numbered as 1, 2, and 3, and embedded in the second-placed section were numbers as 4, 5, and 6 (Figure 2.6). The strains from the setting time through November 3rd are shown in Figure 2.20, and the air temperature was contained in the analysis. The strains of the concrete at early age are shown in Figure 2.20(a), except during the very early age of the cement hydration, the strains at different locations varied in the similar trends as that of the air temperature. On the other hand, the changing rate and range of the strains are different among the different locations. The farther is the distance to the joint, the smaller is the strain. What should be noticed is during the early age of the concrete, the change ranges of the strains in the first section were larger than those in the second section. About two days after the construction of the second section, strains of the same locations in the two sections were almost same.

The concrete strains from November 8th through November 15th are shown in Figure 2.20(b). The analyzed results show that the strains in the two sections cycled as the same trend as the temperature did. The order of the changing rate and range of the strains is the same as that of the early age. And the corresponding strains of first section changed to be smaller than that of second section; the cause of this is that the first section was constructed together with another traffic lane and the second-placed section was constructed separately, which means the construction joint moves more than the warping joint. Except the strains at the center of the slab, the strains at other two locations were negative mostly, which means the concrete shrinkage induced the strain decrease.

The center of VWSG4 was placed at the construction joint, and all the data measured by this gage were illustrated in Figure 2.21 with the air temperature. As shown in the figure, during 4 days after the setting time, the tensile strain increased discontinuously to a large value, which is considered as the effects from the concrete shrinkage mainly. After the early age, the movement of the joint cycled in a large range stably, and was opposite to the changing trend of the air temperature. When the air temperature increased, the concrete expanded and the LCJ closed, and

25

the LCJ opened with the temperature decreased. The range of the joint movement is related to the range of the temperature changing, the larger of the range the temperature changes, the larger the joint moves.
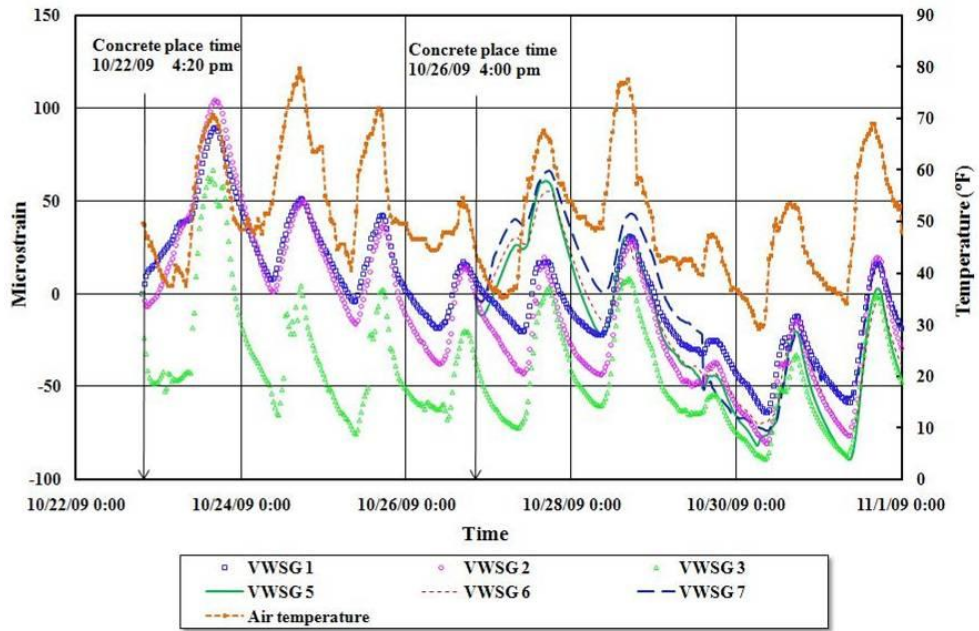


(a) From setting time through November 1st
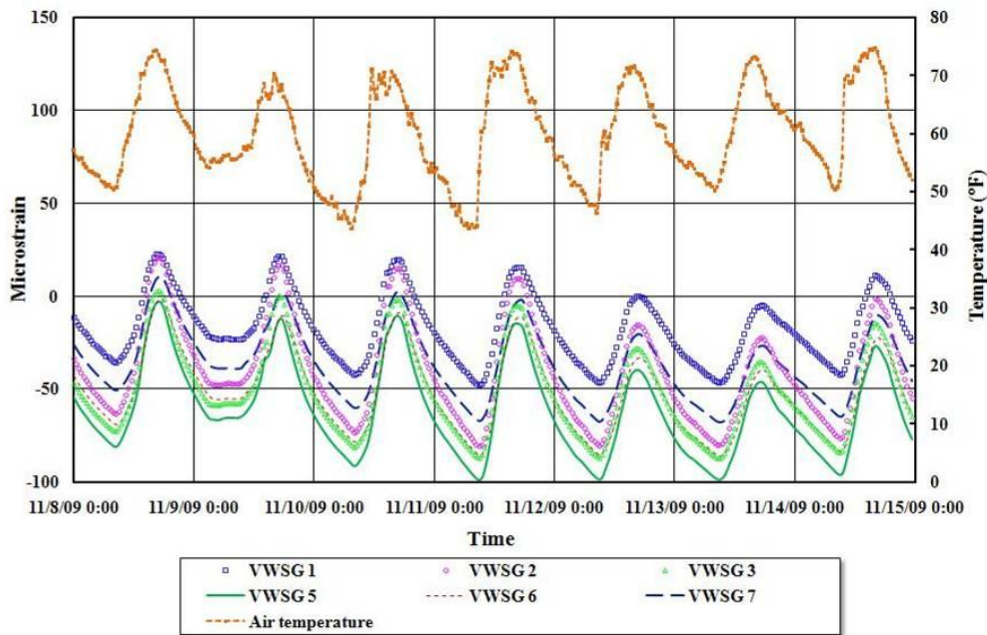


(b) From November 8th through November 15th

*Figure 2.20: Concrete strain*

26
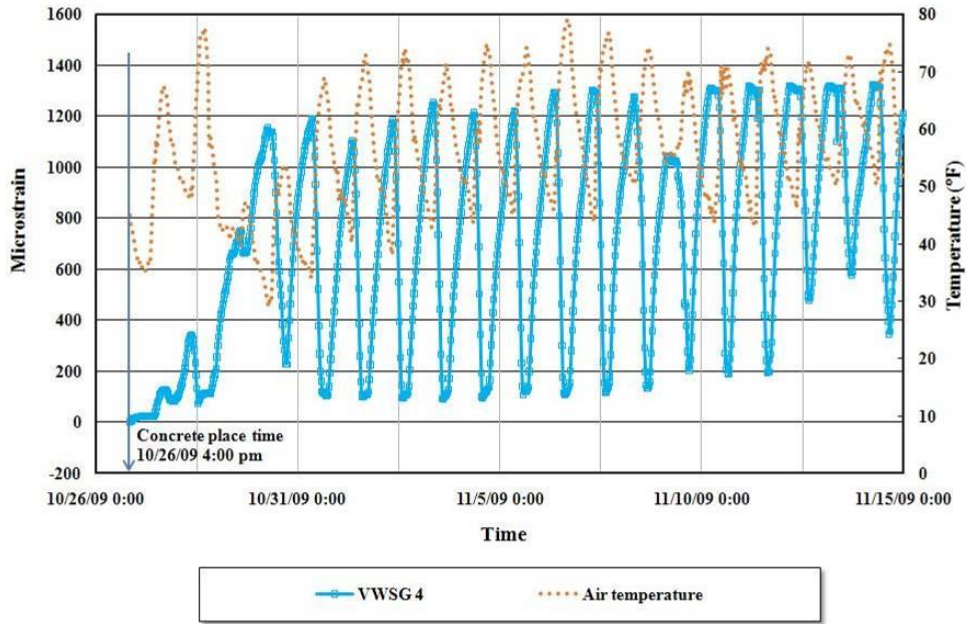
*Figure 2.21: Strain of the gage at the longitudinal construction joint*

0-6190-1

VWSG1: y = 3.0607x - 182.15
VWSG2: y = 3.4423x - 215.75
VWSG3: y = 3.907x - 266.81
VWSG5: y = 4.7039x - 301.34
VWSG6: y = 4.3059x - 273.37
VWSG7: y = 4.1695x - 247.56

(a) ) October 27$^{th}$, 2009



VWSG 1: y = 3.6533x - 249.27
VWSG 2: y = 4.5958x - 328.53
VWSG 3: y = 4.8339x - 357.59
VWSG 5: y = 4.9942x - 375.95
VWSG 6: y = 4.5609x - 340.17
VWSG 7: y = 4.1362x - 295.47
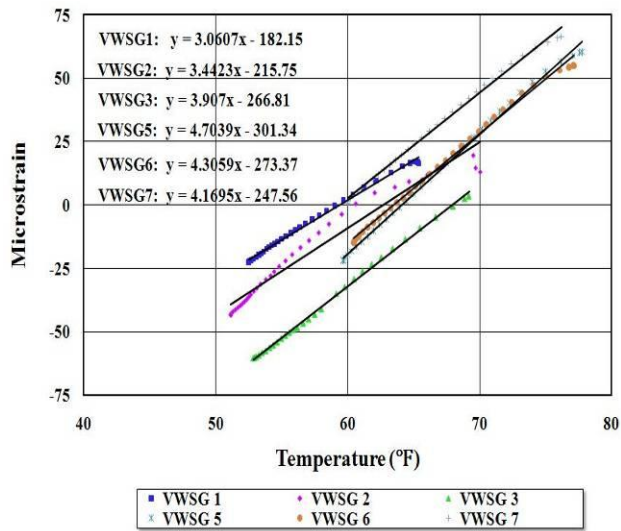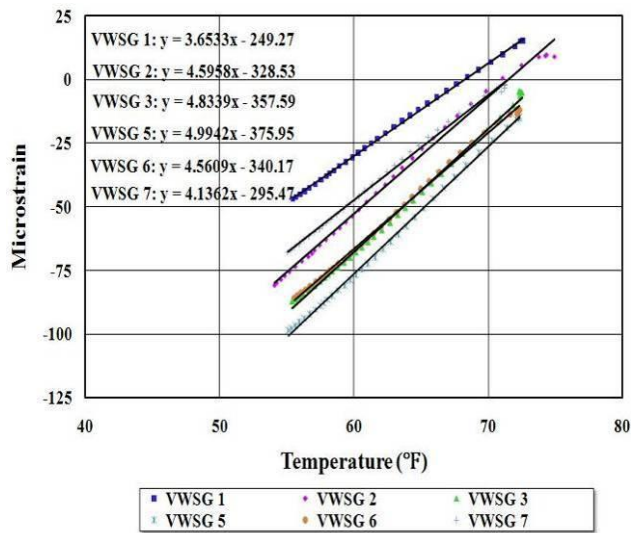
(b) November 12$^{th}$, 2009

*Figure 2.22: Relationship between concrete strain and temperature*

In order to get the relationship between the concrete strains with the air temperature, the data of cooling stage of different ages were analyzed and the trend lines and the slopes are shown in

28

Figure 2.22. Figure 2.22(a) is about the behaviors of October 27$^{th}$, the trend line slopes of the first-placed section are larger than those of the second-placed section, which present the effect of the concrete shrinkage at the early age. With the effect of the concrete shrinkage decreased over time, the trend line slopes became to be similar, which can be seen in Figure 2.22(b). On the other hand, an order exists in the trend line slopes of the two sections. The order from small to big is VWSG1, VWSG2, and VWSG3, and VWSG7, VWSG6, and VWSG5, which means the non-temperature factors which constrained the movement of the concrete increases with the distance to the distance to the construction joint.

*Strain of the tie bar*

Since the SSG are very sensitive, we only got the data from four SSGs, fortunately, three of them were on the same tie bar A. The data of the SSGs had been analyzed from the setting time of the concrete. Because some data of the first 4 days were odd and unstable, hence they were not included in the analysis. The normal SSG data and the air temperature are illustrated in Figure 2.23. The data show the steel was in a compressive state and the strains cycled in an opposite trend of the air temperature changed. The order from small to large is a, b, and c, which means the movement of the tie bar is largest at the location near to the joint, and is smallest at the end. The steel strain at the location near to the joint is as similar as the strain of the concrete at this location, which can verify the bond condition between the steel and the concrete.
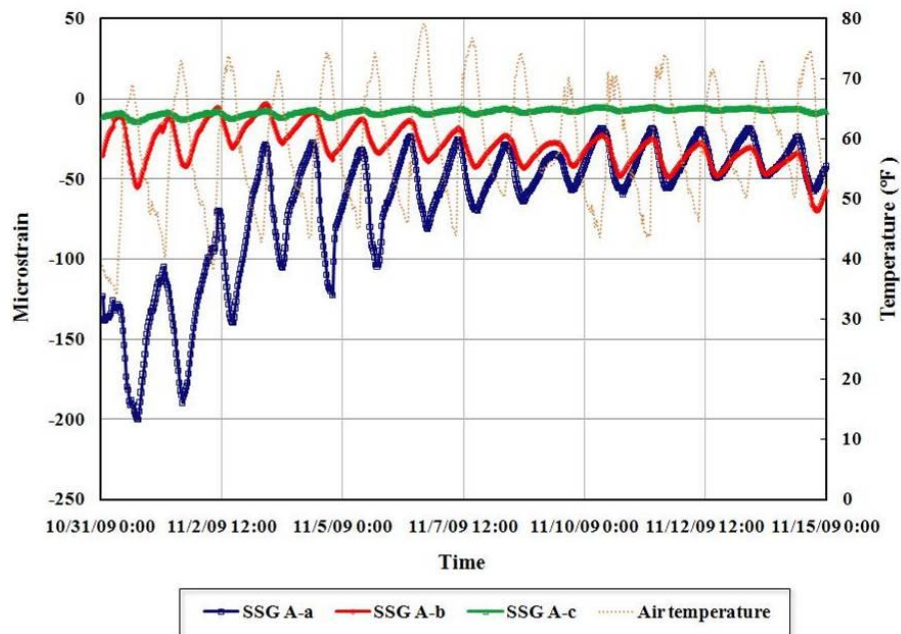


*Figure 2.23: Strain of tie bar at A location*

## 2.3.2 Tie bar stresses

Figure 2.24 illustrates temperature variations at various depths from the placement of the concrete in the Rosenberg section. It shows that maximum concrete temperatures occurred at midnight on the day of concrete placement. It also shows a relatively large difference in concrete temperatures at various depths, even though they diminished with time as the heat of hydration dissipated. The maximum temperature changes occurred near the top of the slab, with the smallest temperature variations near the bottom of the slab.
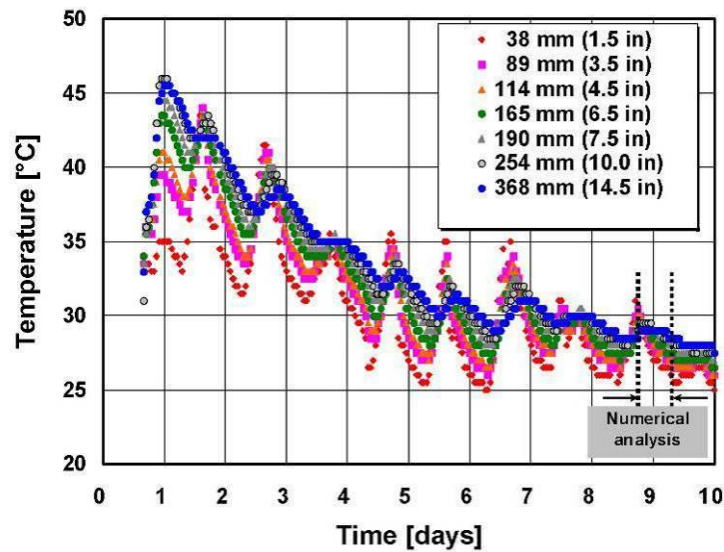


*Figure 2.24: Measured concrete temperature*
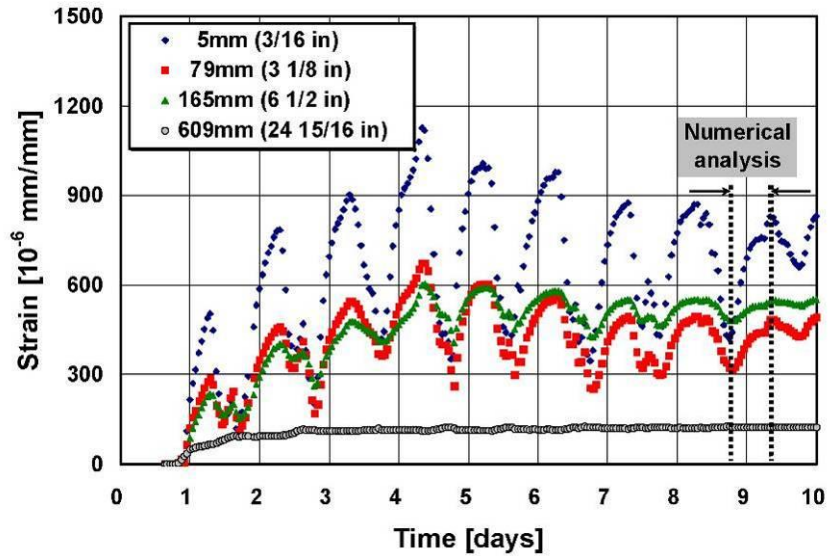
*Figure 2.25: Measured steel strain*

Figure 2.25 shows strains in a tie bar for 10 days after concrete placement at different locations from the LCJ. The numbers in the key indicate the locations of the steel strain gages in terms of distance from the LCJ. As expected, the maximum strains occurred in a gage installed near the LCJ, and very low strains were noted at the end of the tie bar. Maximum strains occurred in mornings, and minimum strains occurred in late afternoon. There is also a rather rapid decrease in steel strain as it moves away from the LCJ, which implies potential bond-slip between tie bars and concretes in the region between 3/16 and 3⅛ in. from the LCJ. However, little difference is noted in steel strains in the region between 3⅛ and 6½ in. from the LCJ. For further theoretical analysis, the data from the evening of Day 8 to early morning of Day 9 were selected and detailed analysis results will be presented in Chapter 3.
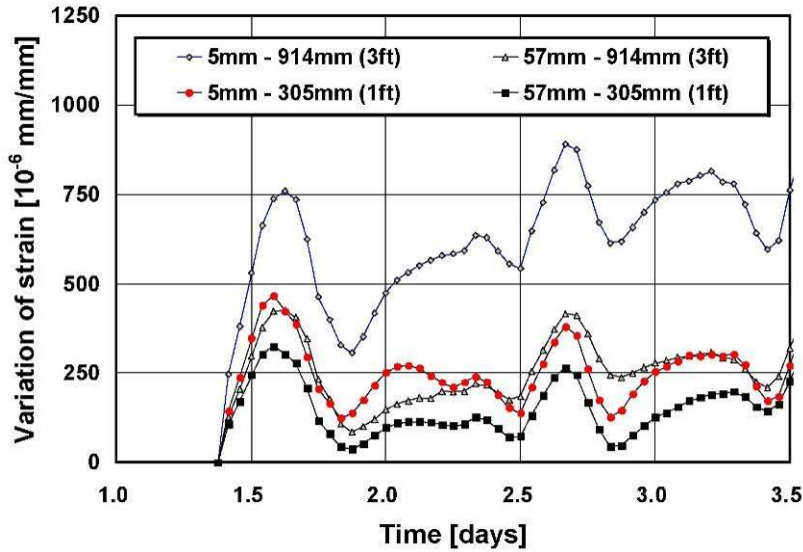
*Figure 2.26: Effect of tie bar spacing on tie bar strain at different distances from LCJ*
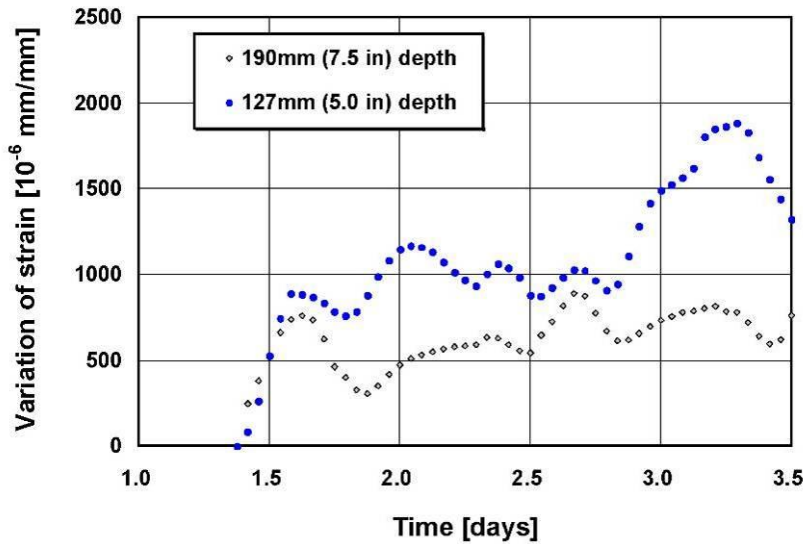


*Figure 2.27: Effect of tie bar depth on tie bar strain*

Figure 2.26 shows strains in tie bars spaced at 1 and 3 ft. In the key, the first number denotes the distance of the measured steel strain from the LCJ and the second number is tie bar spacing. Much greater steel strain was measured at the LCJ in a tie bar with 3-ft spacing than at the LCJ in a tie bar with 1-ft spacing. This result was expected, as more closely spaced tie bars have more

steel cross-sectional area per unit length of concrete slab, which will result in lower steel stress.

Figure 2.27 shows strains in tie bars placed at two depths. Steel strain gages were installed 3/16 in. away from the LCJ. One was placed 5 in. from the top of the slab, and the other was placed 7½ in. from the concrete surface. Strain values were larger in a tie bar placed 5 in. from the concrete surface. These two bars were within 12 ft, and the only difference was in the vertical location of the tie bars.

Figure 2.28(a) indicates the measured temperature profiles from evening on Day 8 (6:00 p.m.; 8¾ days) to morning on Day 9 (8:00 a.m.; 9⅓ days), as shown in Figure 2.24. As expected, the temperature at the top surface of the slab decreased significantly and the decrease declined as the depth increased. Figure 2.28(b) shows the temperature gradient obtained from the measured temperature profiles, which will be applied to the numerical analysis in Chapter 3. This period was selected in the analysis because the change in mechanical properties such as elastic modulus was relatively small compared with the values in the early stages. For the analysis, it was assumed that the changes in material properties during the analysis could be negligible and the error associated with this assumption is quite small.
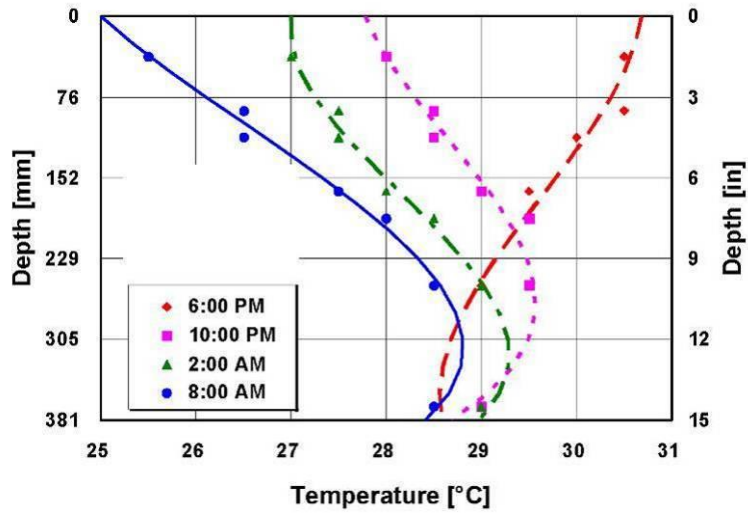
(a) Measured temperature profile at concrete slab from 8¾ to 9⅓ days
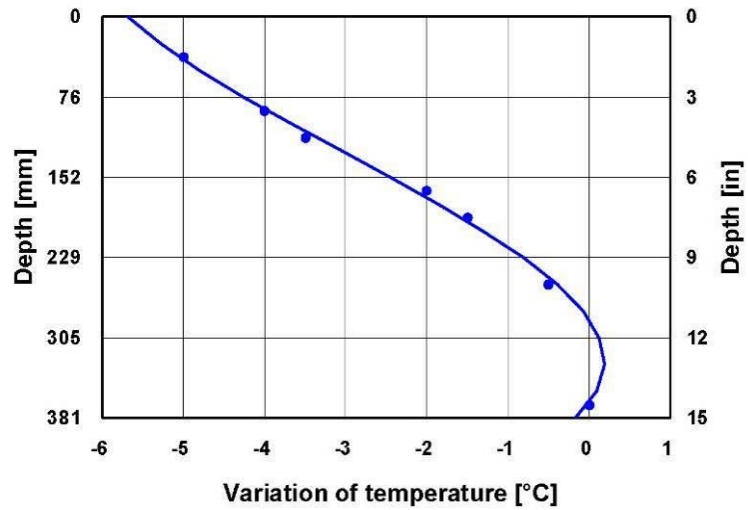


(b) Temperature gradient

*Figure 2.28: Temperature profile and gradient*

Figure 2.29 shows temperature variations at various depths in the Rosenberg and Fort Worth sections. Figure 2.30 shows the variations of tie bar strain at different distances from the LCJ. The relationship between change in average temperature of concrete and change in tie bar strain was analyzed. The data from evening to early morning of the next day were selected as shown in

34

Figures 2.29 and 2.30. The concrete maturity at the sixth day in the Rosenberg section was similar to that at the eighth day in the Fort Worth section.
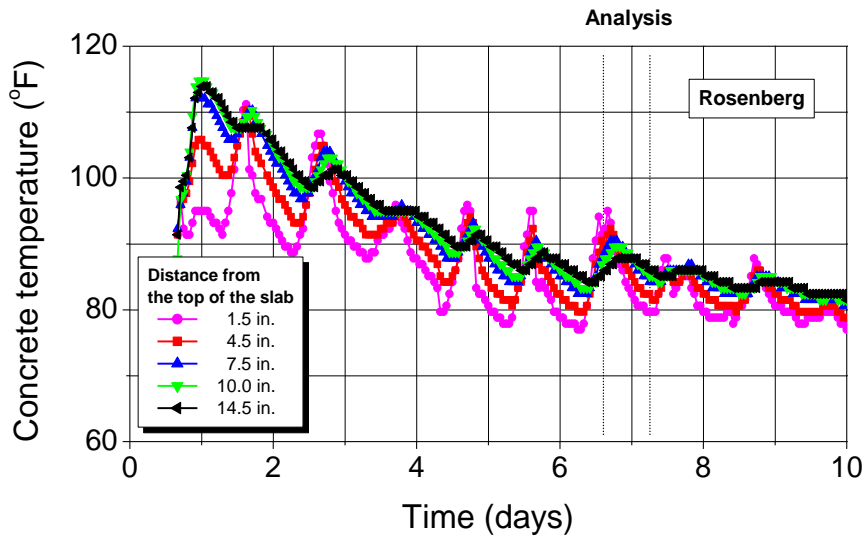


(a) Rosenberg section
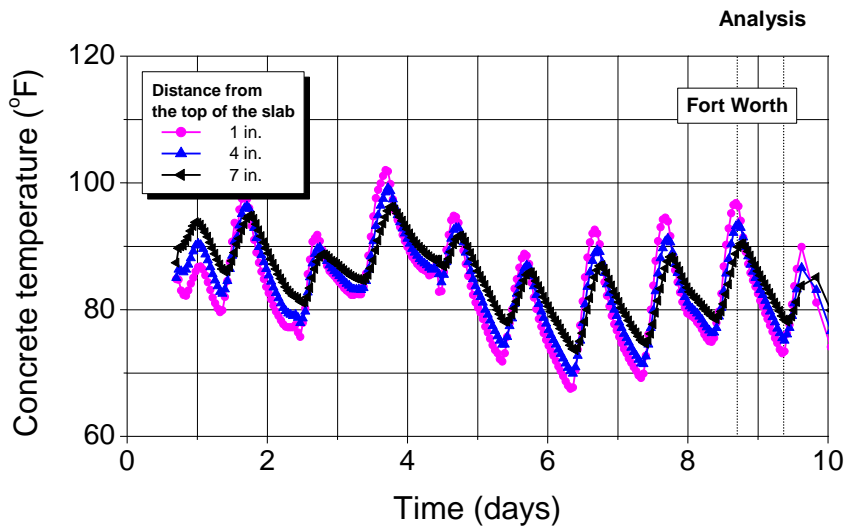


(b) Fort Worth section

*Figure 2.29: Variation of concrete temperature*

0-6190-1
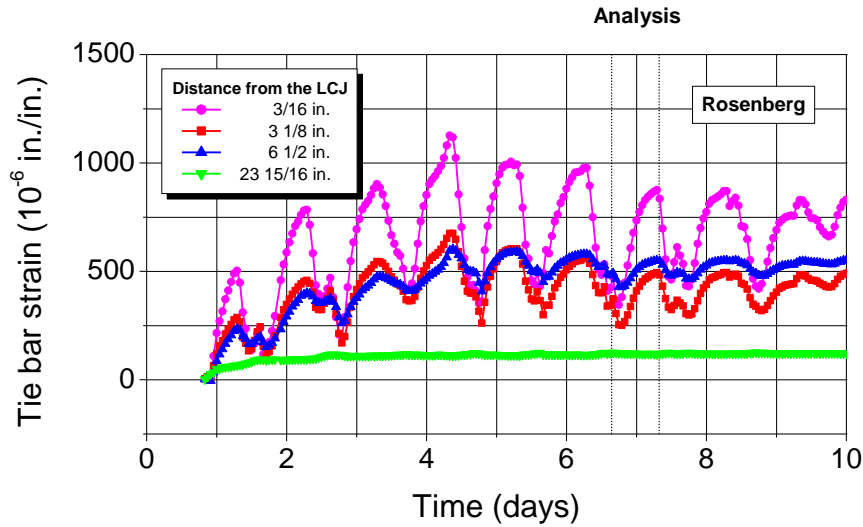
(a) Rosenberg section
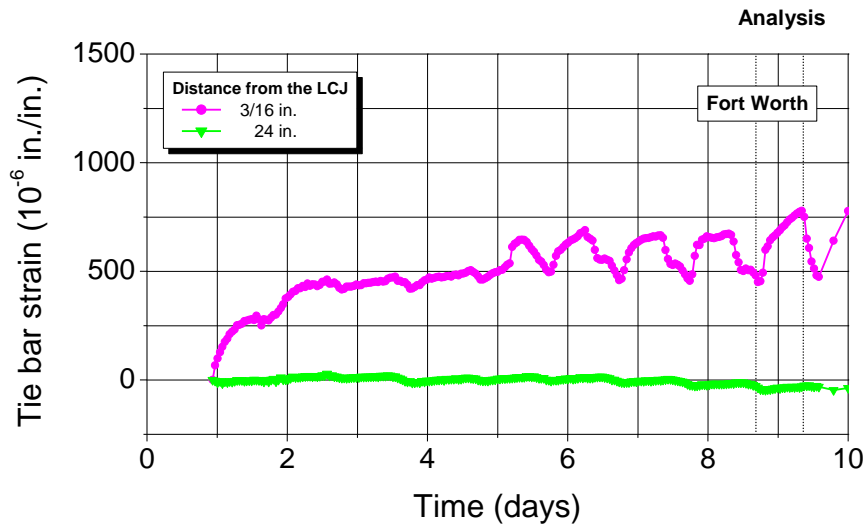


(b) Fort Worth section

*Figure 2.30: Variation of tie bar strain*

In Figure 2.31, the *x*-axis denotes the change in the average temperature of concrete after the evening of the selected day and the *y*-axis denotes the change in the tie bar strain at a distance of 3/16 in. from the LCJ. A same amount of decrease in the average concrete temperature resulted in a larger increase in the tie bar strain in case of the Rosenberg section where the pavement was thicker and wider. This is likely because the nonlinearity of the thermal gradient along the depth

36

axis becomes more severe as the pavement is thicker and the axial movement of pavement due to temperature change is greater as the pavement is wider. It can be inferred from the result that the concrete stress will also be influenced by pavement geometries because it depends on the restraint provided by tie bars.
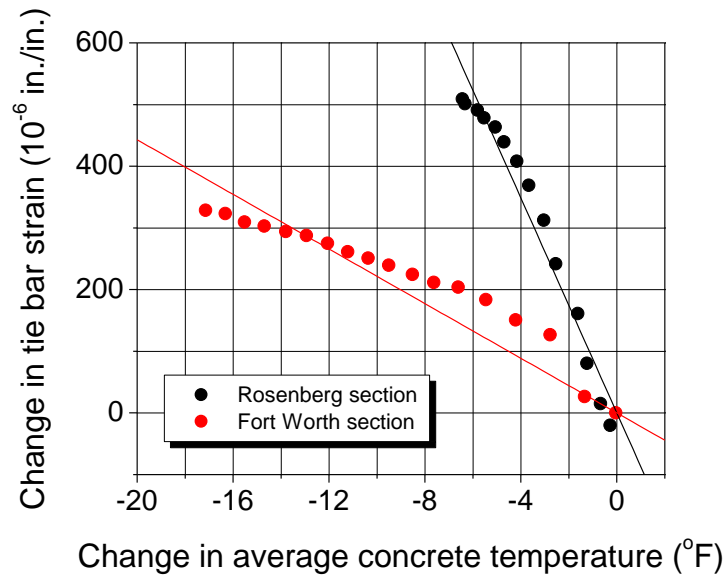


*Figure 2.31: Change in average concrete temperature vs. change in tie bar strain*

## 2.4 Summary

Field testing was conducted in several new CRCP construction projects in Texas to investigate the behavior of concrete pavements and to provide useful information for the verification of numerical model. Steel strain gages were installed at different locations in tie bars to measure tie bar stresses due to environmental loadings. Concrete strain gages were installed at the top of the slab at different distances from the LCJ in the transverse direction and concrete displacement gages were installed across the LCJ in the transverse direction. These gages were installed in each test section – tied section and doweled section – to investigate the difference in the behavior of tied CRCP and doweled CRCP. The following conclusions, based on field experiments, were reached: (1) concrete temperatures evaluated at various depths from the concrete placement showed substantial variations through the slab depth; (2) the temperature gradient along the depth of the slab showed a character of nonlinear distribution; (3) the opening of the LCJ at the early age resulted from the drying shrinkage of the concrete mainly; (4) after the early age, the movement of the LCJ cycled in a large range stably, and was opposite to the changing trend of the air temperature; (5) the construction joint moved more than the warping joint; (6) concrete elements were more restrained as it gets close to tie bars in the vertical direction; (7) the

movement of concrete at LCJ was larger in the doweled section than in the tied section; (8) larger transverse concrete stress developed farther away from the LCJ; (9) larger transverse concrete stress developed in the tied section than in the doweled section; (10) tie bar stresses increased rapidly as it gets close to the LCJ; (11) much higher stresses were developed in a tie bar placed closer to the slab surface; and (12) lower tie bar stresses developed as tie bars were placed more closely.

0-6190-1

# CHAPTER 3 DEVELOPMENT AND VERIFICATION OF NUMERICAL MODEL

In Portland cement concrete pavement, tie bars are installed at LCJs primarily to keep the lanes together and secondarily to provide load transfer. The design of tie bars is based on subgrade drag theory (SGDT) (Huang, 2004). This theory assumes that no temperature variations exist through the slab depth and therefore the slab displacements in the transverse direction are the same at all depths. Stresses in tie bars are computed from equilibrium between frictional resistance provided by the subbase as the slab displaces due to temperature variations and the forces in tie bars. The spacing for tie bars is determined by limiting the maximum steel stress in tie bars to a prescribed value, usually 75% of the yield strength. Because of the assumptions made in SGDT, tie bar spacing is inversely proportional to the widths of lanes tied together. SGDT is quite simple in concept and easy to implement. However, a number of researchers have shown that the basic assumption made in SGDT – uniform temperature distribution throughout concrete slabs – is not valid (Ghali et al., 2002; Mohamed and Hansen, 1997). Substantial temperature variations exist through slab depth, which will induce displacements in concrete slab in a vertical direction (curling). Figure 3.1 illustrates the decomposition of nonlinear temperature effects by showing three components that result in the equivalent behavior of a concrete slab subjected to nonlinear temperature variations through the slab depth. The first component is the axial strain, which SGDT addresses. SGDT does not consider the other two components (curling strain and nonlinear strain). Ignoring those two components could result in inaccurate estimation of tie bar stresses and unreasonable tie bar designs.



(a) Temperature gradient    (b) Component causing axial strain    (c) Component causing curling strain    (d) Component causing nonlinear strain
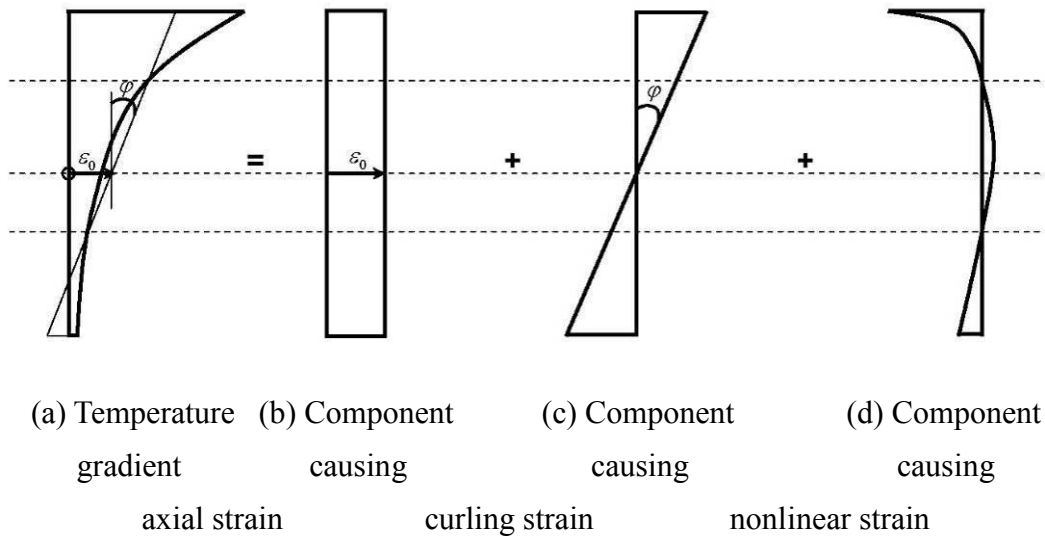
*Figure 3.1: Decomposition of nonlinear temperature effects*

A field experiment was conducted to evaluate concrete displacements in vertical and transverse directions at the free edge. Figure 3.2(a) shows the gage installed for the measurements of

vertical slab displacements, and Figure 3.2(b) illustrates the measured values for 6 days. The slab was 15 in. thick. Figure 3.2(b) clearly illustrates the curling behavior of the concrete slab. The displacements on the *y*-axis decrease if the slab is going down. The slab curled down in late afternoon when top temperatures were higher than bottom temperatures. On the other hand, it curled up in early morning when top temperatures were lower than bottom temperatures. Figure 3.3(a) shows gages installed to evaluate horizontal displacements of the concrete at the free edge. This slab was 15 in. thick. The displacements were measured at three depths of the slab: top (1 in.), middle (7.5 in.), and bottom (14 in.). Figure 3.3(b) illustrates the measurement. On the *y*-axis, as the slab moves toward the free edge, the displacement number increases. For example, in late afternoon, the top at the free edge moved toward the gages, whereas in early morning, it moved away from the gages. The displacements at the top and bottom were moving in nearly opposite directions. The measured vertical and horizontal concrete displacements clearly indicate the existence of curling components in the slab movements. If the assumptions made in SGDT are true, there should be no variations in the vertical displacements in Figure 3.2(b), the transverse displacements at three depths should be parallel to each other in Figure 3.3(b), and the tie bar strains at two depths should be the same in Figure 2.27.
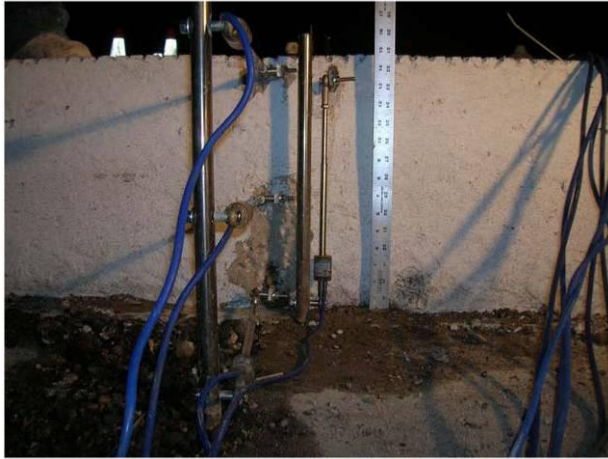
(a) Crackmeter for vertical movement measurements
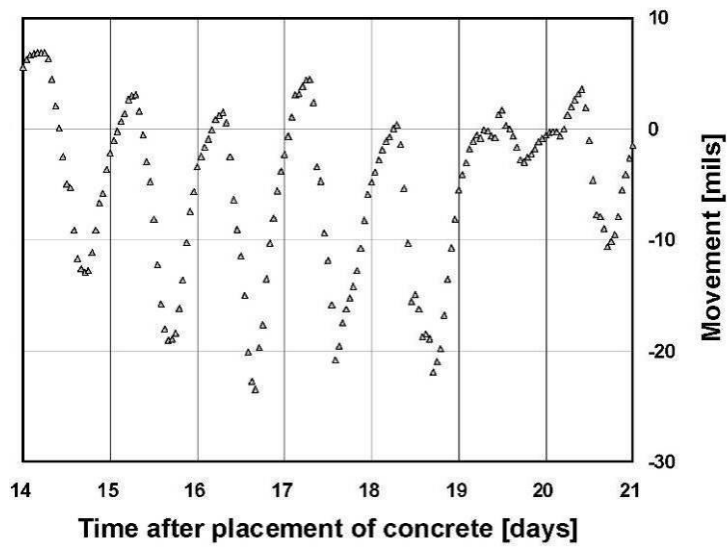


(b) Measured data

*Figure 3.2: Measurement of vertical movement*

(a) Crackmeter for transverse movement measurements
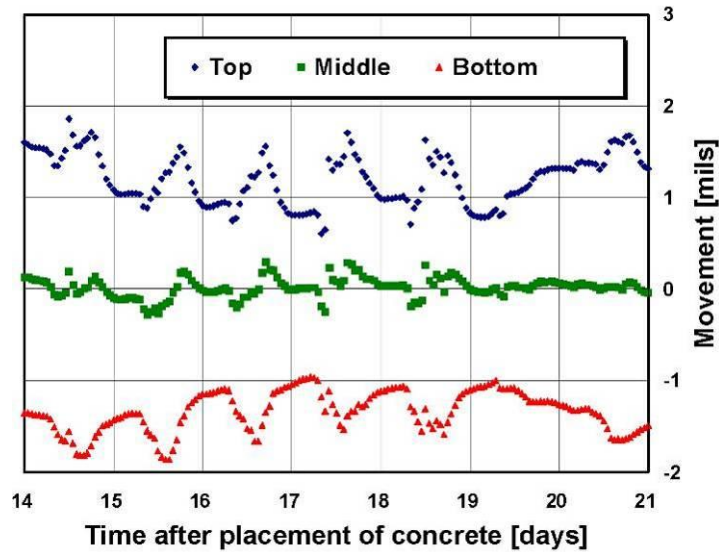


(b) Measured data

*Figure 3.3: Measurement of transverse movement*

This finding indicates that SGDT alone may not be adequate to estimate accurately the stresses that develop in tie bars due to temperature variations in concrete. Rather, more detailed structural analysis is needed with proper input values and a constitutive equation. Also, purely theoretical analysis alone may not be able to predict concrete stresses accurately either. Accordingly, an improved numerical model was developed to analyze a concrete pavement with tie bars at LCJs

42

and its validity was verified with the field data.

## 3.1 Three-Dimensional Finite Element Model

### 3.1.1 Finite element modeling

Figure 3.4 describes the three-dimensional finite element model of a concrete pavement with tie bars (or dowel bars) at LCJs. The numerical analysis was performed with the aid of the commercial finite element analysis program DIANA (Displacement method ANAlyser) ver. 8.1.2 (DIANA, 2003). DIANA is a general purpose finite element code, based on the displacement method. It was developed by civil engineers from a civil engineering perspective in 1972. It has been under development at TNO located in Delft, the Netherlands. DIANA ver. 9.4.2 was recently launched. Civil, mechanical, biomechanical, and other engineering problems can be solved with the DIANA program. Its most appealing capabilities are in the fields of concrete and soil. Standard DIANA application work includes the following: concrete cracking, excavation, tunneling, composites, plasticity, creep, cooling of concrete, groundwater flow, fluid-structure interactions, temperature-dependent material behavior, heat conduction, stability analysis, buckling, phased analysis, substructuring, etc.
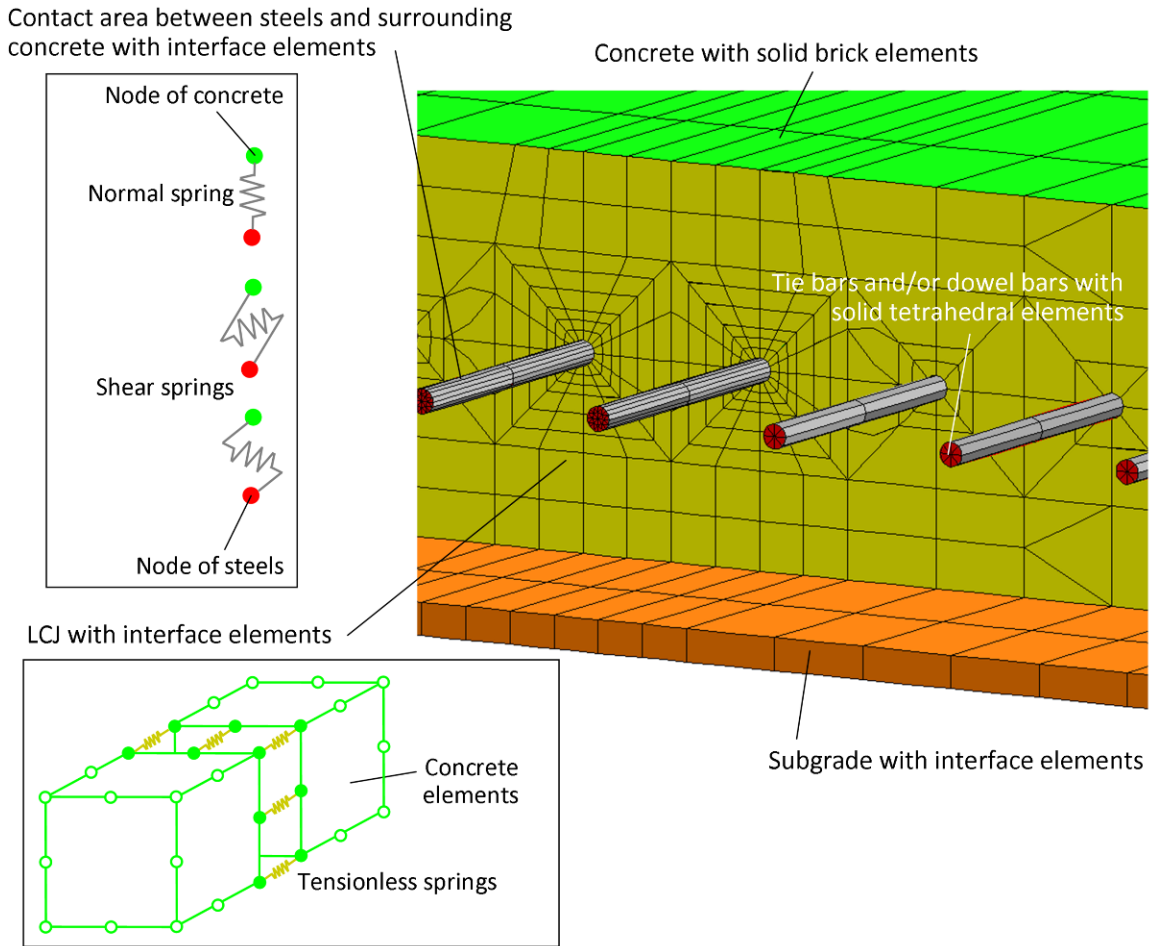
*Figure 3.4: Three-dimensional finite element modeling of a concrete pavement*
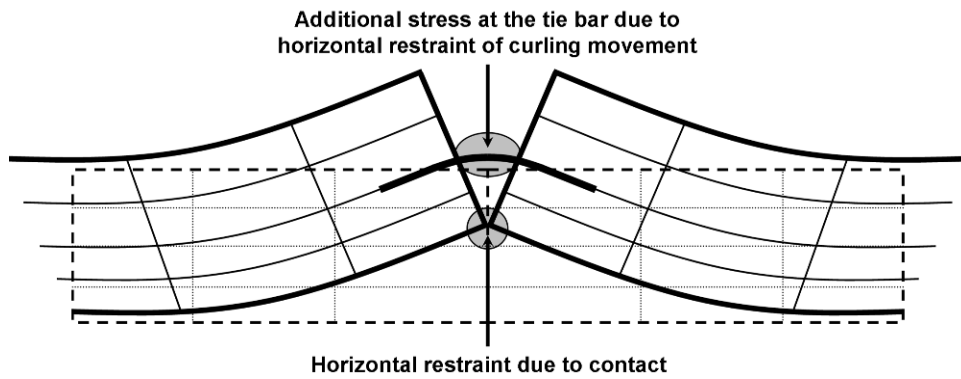


*Figure 3.5: Restraining effect at the bottom of longitudinal construction joint*

44

As shown in Figure 3.4, twenty-node isoparametric solid brick elements were used in the mesh representation of concrete. Fifteen-node isoparametric solid wedge elements were used in the mesh representation of tie bars and dowel bars. The interactions between steels and surrounding concrete were considered by modeling their contact area using 8+8-node plane quadrilateral interface elements. The interface element, which is equivalent to a series of spring elements, was placed between the faces of concrete and steel elements. Although the faces of concrete and steel elements have the same coordinate values, – the interface element has zero-thickness – they are definitely separate faces connected by the interface element. The interface element defines a relation between tractions and relative displacements across the interface. These have normal and shear components. The relation between shear traction and shear relative displacement describes bond-slip behavior between steels and surrounding concrete. The relation between normal traction and normal relative displacement describes debonding behavior.

Subgrade was modeled with plane quadrilateral interface elements. The relation between normal traction and normal relative displacement describes the vertical stiffness of subgrade. The relation between shear traction and shear relative displacement characterizes friction-slip behavior between concrete and subgrade. As shown in Figure 3.5, if a pavement bends upward due to a negative nonlinear thermal gradient, two adjacent lanes would restrain each other at the bottom of the LCJ. To consider this restraining effect, the LCJ was modeled with tensionless plane quadrilateral interface elements with sufficient stiffness in compression.

### 3.1.2 Verification of numerical model

To verify the validity of the numerical model, numerical results were compared with the measured data. As previously mentioned in Section 2.1.1.1, the field testing was conducted in a new CRCP construction project in Belton. Figure 3.6 shows the geometric configuration of the test section. The pavement was 14 in. thick. The existing slab was 36 ft wide and composed of one inside shoulder and two lanes. A new 22 ft-wide slab was placed with a LCJ in between on 4 inch-thick asphalt layer. The new slab was saw-cut dividing into a lane and an outside shoulder. The overall slab had three LCJs and one longitudinal warping joint (LWJ). Two layers of transverse steel with a diameter of 0.75 in. were placed and their spacing was 1.5 ft. Upper and lower transverse steels were placed one after the other. Dowel bars were placed in lieu of tie bars in a certain part of the slab. The diameters of tie bars and dowel bars were 0.75 and 1 in., respectively. The half-lengths of tie bars and dowel bars were 25.0 and 10.5 in., respectively.
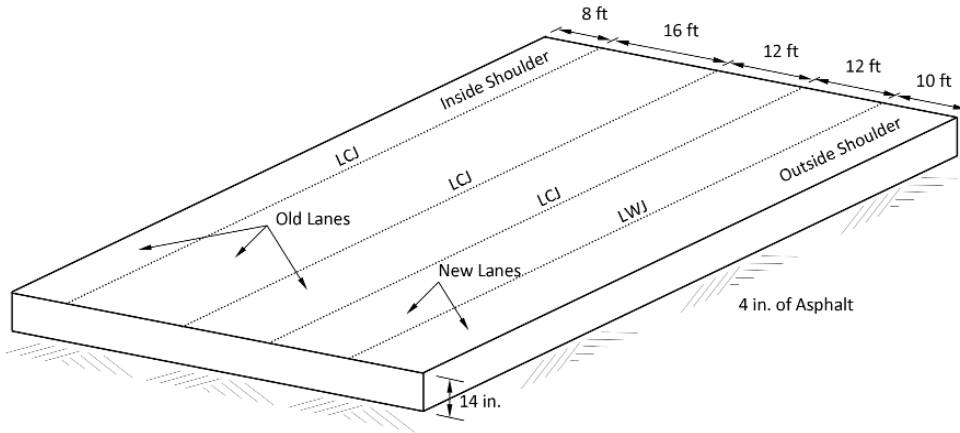
(a) Geometric configuration of the test section
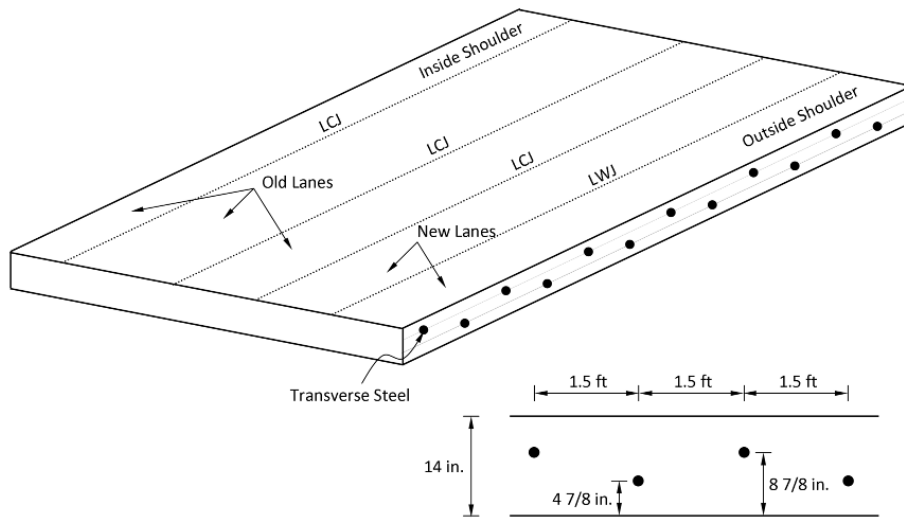


(b) Layout of transverse steels
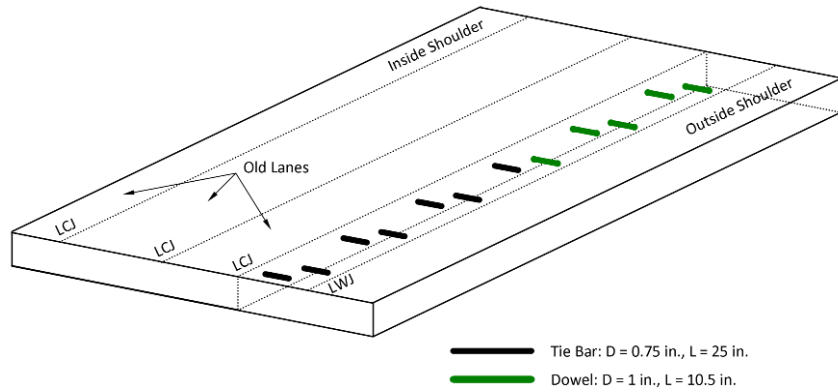


(c) Layout of tie bars and dowel bars

*Figure 3.6: CRCP construction project in Belton*

46

Figure 3.7 shows the finite element mesh discretization of the tied and doweled sections of the slab. Only 1.5 ft-long portion of the slab, which includes half of an upper tie bar (or dowel bar) and half of a lower tie bar (or dowel bar), was modeled and two cutting planes were restrained in the longitudinal direction, in a similar manner to plane strain analysis.
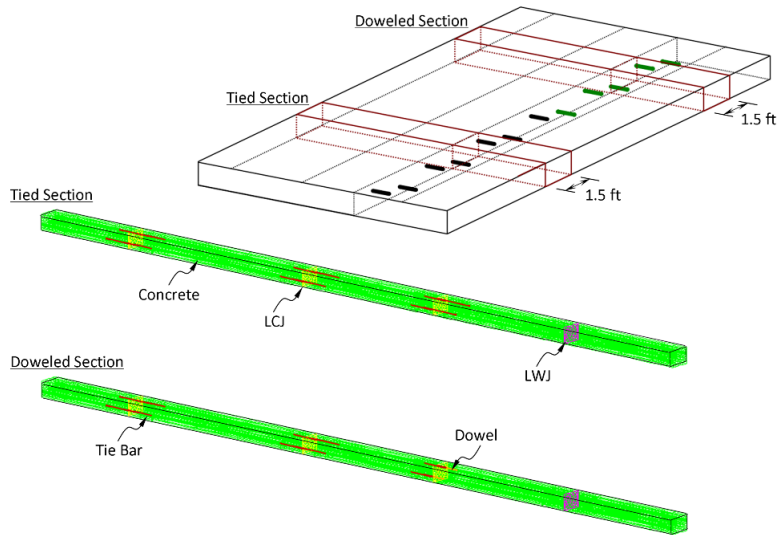


(a) Finite element mesh discretization of the tied and doweled sections
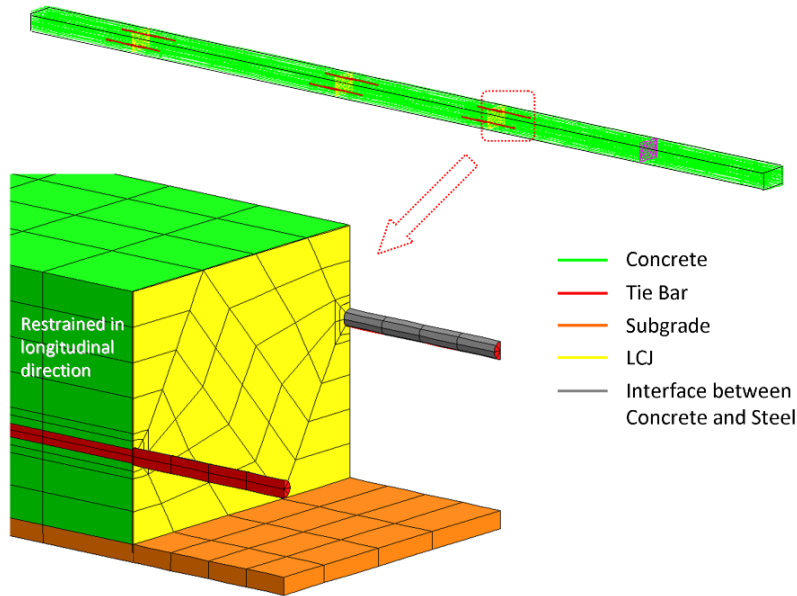


(b) Zoomed-in shaded view

*Figure 3.7: Finite element mesh model*

The measured elastic modulus and CTE of concrete were $5.18 \times 10^6$ psi and $4.22 \times 10^{-6}$ /°F during the specified period from afternoon of Day 82 to morning of Day 83 (see Section 2.3.1.1). The elastic modulus and CTE of steel were assumed to be $2.9 \times 10^7$ psi and $6.4 \times 10^{-6}$ /°F. The Poisson's ratio of concrete and steel were assumed to be 0.15 and 0.30, respectively. The bond-slip behavior between tie bars and surrounding concrete was characterized using plane interface elements with the relation between shear traction and shear relative displacement, as shown in Figure 3.8 (Kim et al., 2000). A large stiffness was assigned to the relationship between normal traction and normal relative displacement to keep the debonding between tie bars and concrete to a minimum. The bond strength between dowel bars and concrete was assumed to be zero. The modulus of subgrade reaction was assumed to be zero in tension and 500 psi/in. in compression. The friction-slip behavior between concrete and subgrade was characterized using plane interface elements with the relation between shear traction and shear relative displacement, as shown in Figure 3.9 (Kim et al., 1997). It was assumed that cracks did not develop at the LWJ contrary to expectations. Temperature gradient represented in Figure 2.15(b) was applied to the slab.
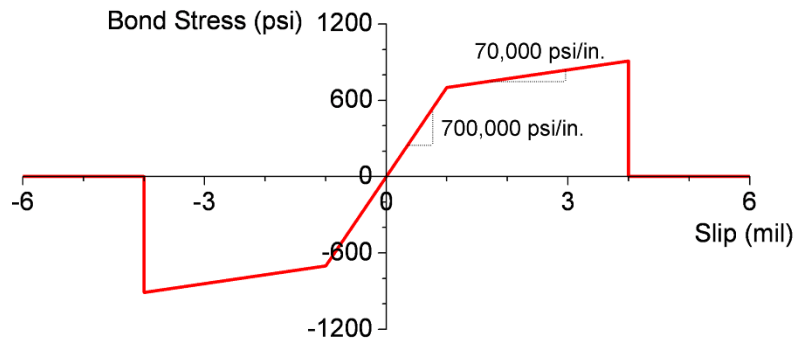


*Figure 3.8: Bond-slip behavior between tie bars and surrounding concrete*
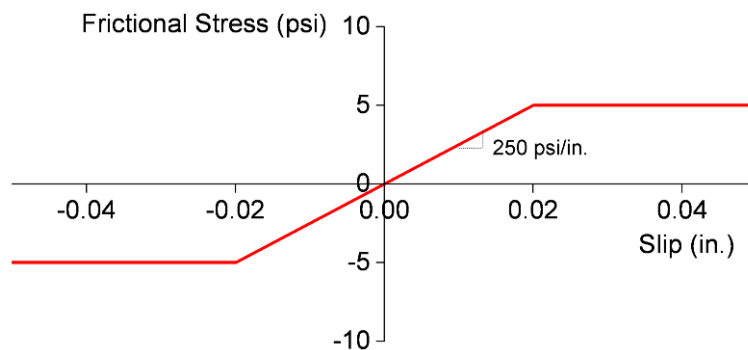


*Figure 3.9: Friction-slip behavior between concrete and subgrade*

Figure 3.10 illustrates the deformed shape and surface deflection of the tied and doweled sections. The difference in surface deflection between the two sections is relatively large near the LCJ between the existing and new slabs. The surface deflection at the LCJ is larger in the doweled section than in the tied section. Figure 3.11 shows the transverse displacement across the LCJ between the existing and new slabs (see Figure 2.11). As expected, the lane separation is larger in the doweled section. The lane separation is a little smaller above the upper tie bar than above the lower tie bar. This is because the closer a tie bar placed to the top of the slab, the more it restrains the movement of concrete elements at the top of the slab. The numerical results and measured data show favorable agreement.
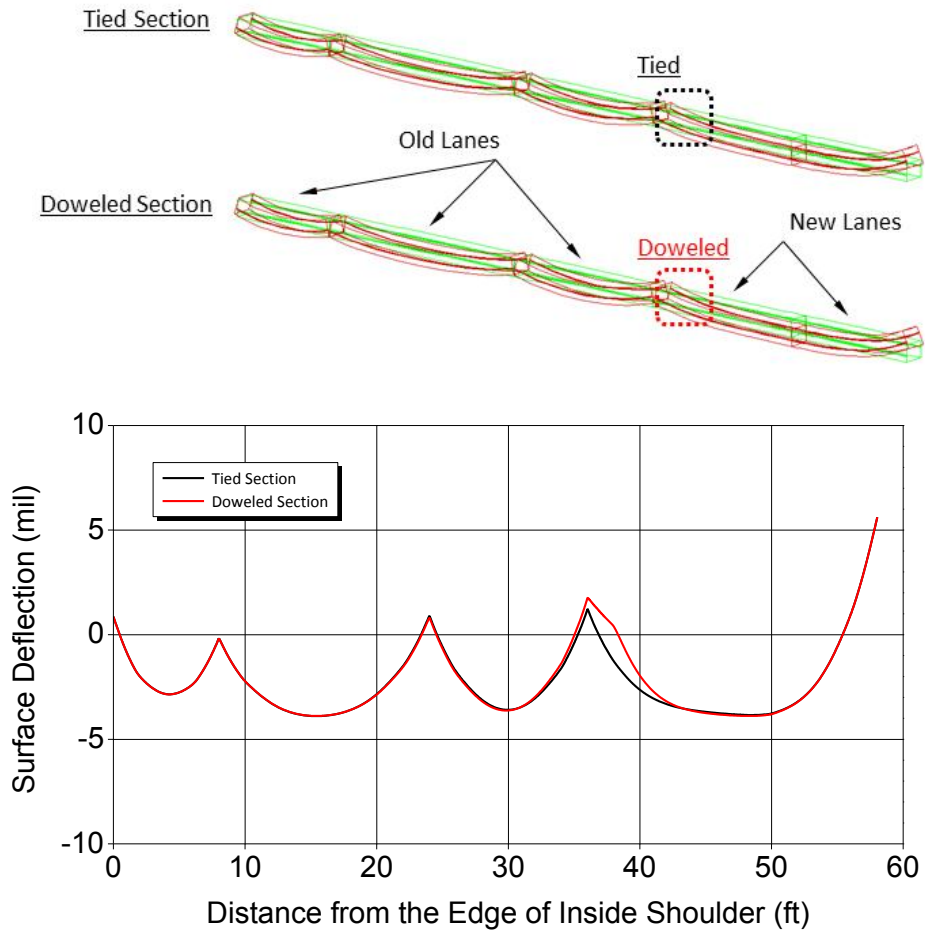


*Figure 3.10: Deformed shape and surface deflection*
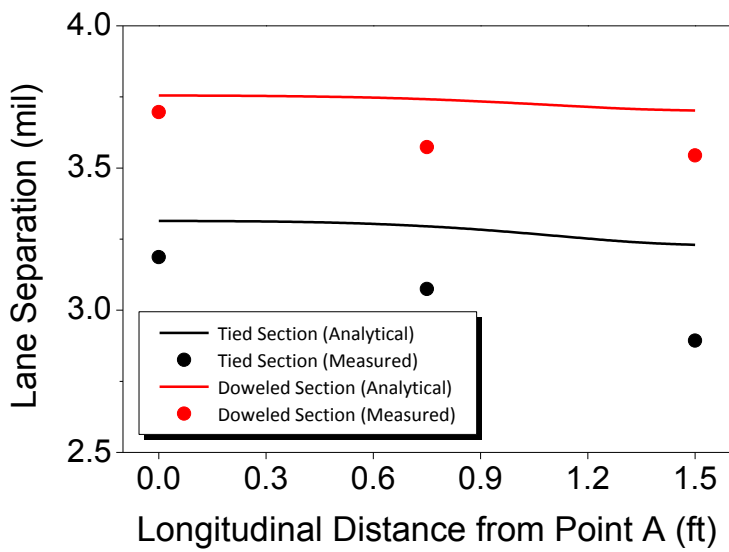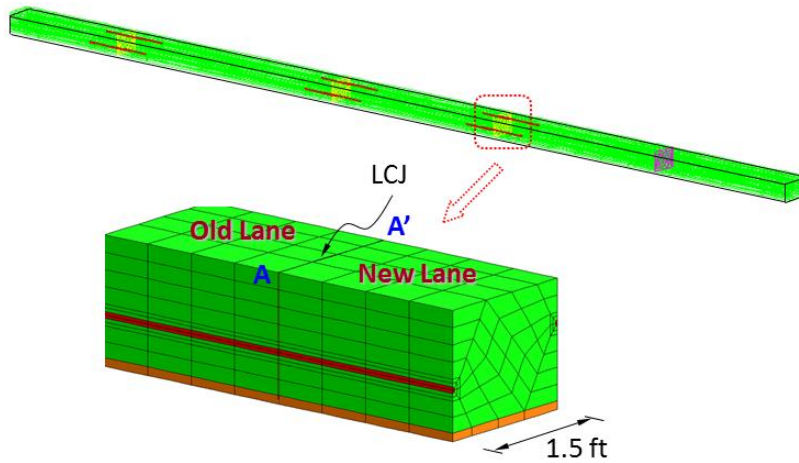
*Figure 3.11: Transverse displacement across the LCJ between the existing and new slabs*
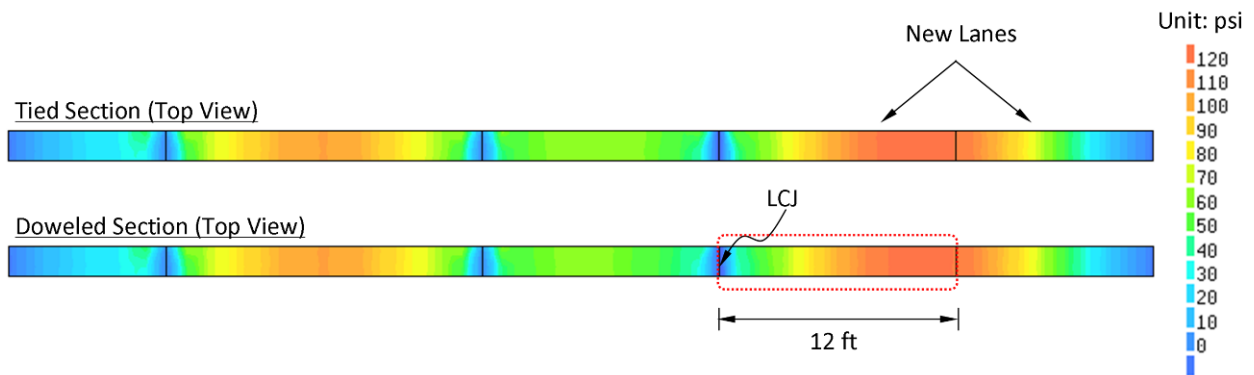


*Figure 3.12: Transverse concrete stress at a depth of 1 in.*
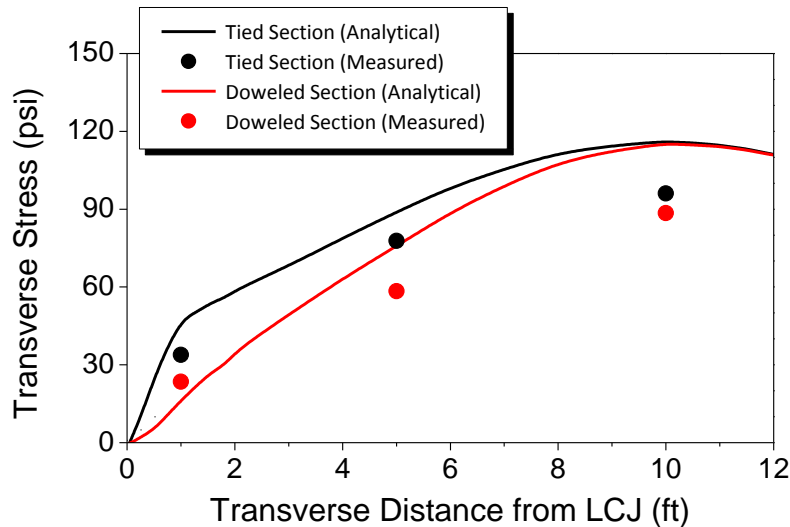
*Figure 3.13: Transverse concrete stress in the outermost driving lane*

Figure 3.12 shows the distribution of transverse concrete stress at a depth of 1 in. Tensile stresses develop in general but it decreases to zero when approaching the LCJs. The maximum stress in each lane occurs in the middle of the lane and its magnitude increases as the lane width increases. In the new slab, the maximum stress occurs near the LWJ because it was assumed that cracks did not develop at the LWJ. Figure 3.13 shows the transverse concrete stress in the outermost driving lane (see Figure 2.17). The stresses in this figure were calculated in the middle of two adjacent transverse steels and at a depth of 1 in. Larger stresses develop farther away from the LCJ because the movement of concrete is more restrained in the middle of the slab. Larger stresses occur in the tied section than in the doweled section because tie bars provide more restraints in transverse direction. However, the difference diminishes as it gets close to the LCJ. Considering the uncertainty in the material properties used in the analysis, the numerical results show favorable agreement with the measured data.

**3.2 Two-Dimensional Finite Element Model**

**3.2.1 Finite element modeling**

In the previous section, a three-dimensional finite element model of a concrete pavement with tie bars (or dowel bars) at LCJs was developed and verified with the field data. However, modeling the bars with three-dimensional solid elements significantly increase the total number of finite elements because it requires the use of a very refined mesh. Three-dimensional finite element analysis with a large number of solid elements is very time-consuming, and in the worst case, it may not be able to run the program due to insufficient memory. Accordingly, a two-dimensional

0-6190-1

finite element model – a simplified model which uses plane strain elements for modeling concrete – is introduced to analyze a concrete pavement with tie bars (or dowel bars) at LCJs and verified with the measured data. The simplified model is possible because CRCP is sufficiently long with repeated geometry and it is subjected to environmental loading only in this analysis – temperature gradients do not change along the longitudinal axis. For verification purpose, a simple reinforced concrete tension member was analyzed with both three-dimensional and plane strain models, and the results showed little difference.

Figure 3.14 shows the two-dimensional finite element model of concrete pavement with the tie bar (or dowel bar) at the LCJ. The numerical analysis was performed with the aid of the commercial finite element analysis program DIANA ver. 8.1.2. Eight-node quadrilateral isoparametric plane strain elements were used in the mesh representation of concrete. Two-dimensional beam elements were used in the mesh representation of tie bars and dowel bars. Subgrade was modeled with 3+3-node line quadrilateral interface elements, which are equivalent to a series of normal and shear spring elements. The relation between normal traction and normal relative displacement describes the vertical stiffness of subgrade. The relation between shear traction and shear relative displacement characterizes friction-slip behavior between concrete and subgrade.
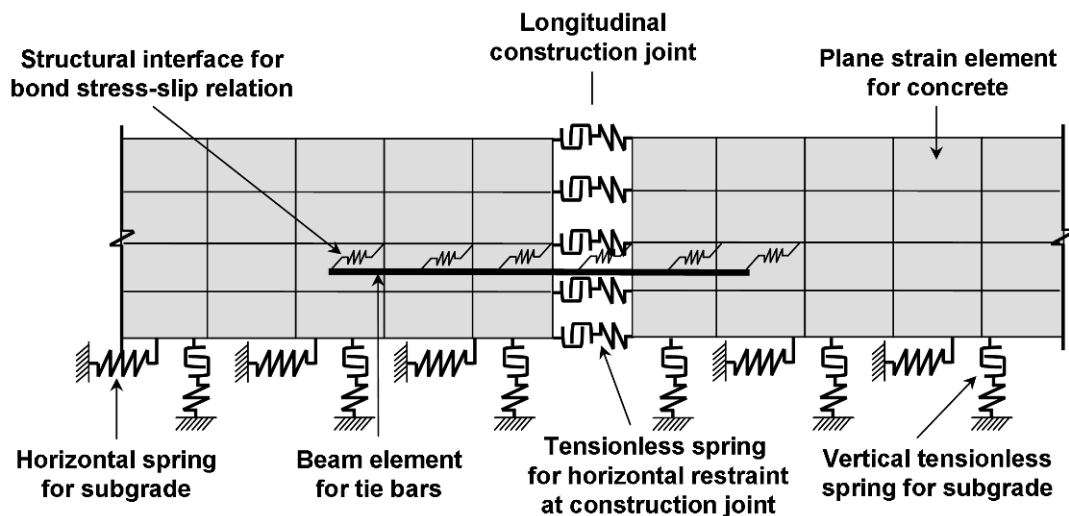


*Figure 3.14: Two-dimensional finite element modeling of a concrete pavement*

The interactions between steels and surrounding concrete were considered by modeling their contact area using 3+3-node line quadrilateral interface elements. The interface element, which is equivalent to a series of normal and shear spring elements, was placed between the concrete and steel elements. The relation between shear traction and shear relative displacement describes bond-slip behavior between steels and surrounding concrete. The relation between normal traction and normal relative displacement describes debonding behavior. The top and bottom portions of concrete may contract and expand, respectively, depending on the degree of

nonlinearity of the temperature gradient. As shown in Figure 3.5, when the slab tries to expand at the bottom, another slab restrains it. To consider this restraining effect, the LCJ was modeled with tensionless line quadrilateral interface elements with sufficient stiffness in compression.

**3.2.2 Verification of numerical model**

To verify the validity of the numerical model, numerical results were compared with the measured data. As previously mentioned in Section 2.1.2, the field testing was conducted in a new CRCP construction project in Rosenberg. The pavement was 15 in. thick. Number 6 tie bars with a length of 24.0 in. were placed at 3-ft spacing. In the numerical analysis, CTEs for the concrete and tie bar were assumed to be $4.0 \times 10^{-6}$ and $6.4 \times 10^{-6}$ /$^{\circ}$F, respectively. The elastic modulus of the tie bar was assumed to be $2.9 \times 10^{7}$ psi. On the basis of CEB-FIP Model Code 1990 (CEB, 1993), development of elastic modulus with time was estimated from 28 days of compressive strength (5,000 psi) and the maturity function that considers the effect of temperature on the process of development of hydration. Average temperature was used to calculate the concrete's maturity. Poisson's ratios of tie bar and concrete were assumed to be 0.3 and 0.15, respectively.

The bond-slip behavior between tie bars and surrounding concrete was characterized using line interface elements with the relation between shear traction and shear relative displacement, as shown in Figure 3.8 (Kim et al., 2000). A large stiffness was assigned to the relationship between normal traction and normal relative displacement to keep the debonding between tie bars and surrounding concrete to a minimum. The modulus of subgrade reaction was assumed to be zero in tension and 400 psi/in. in compression. The frictional stress-slip stiffness was assumed to be 150 psi/in. with a yield-slip of 0.02 in. Temperature gradient represented in Figure 2.28(b) was applied to the slab.

Figure 3.15(a) shows the distribution of tie bar stress variation from the numerical analysis along the tie bar from the LCJ. The dotted line represents predicted tie bar stress solely due to the axial component in concrete slab displacements shown in Figure 3.1. The solid line shows the predicted tie bar stress due to the combined effects of the three components shown in Figure 3.1. There is good agreement between the predicted and measured tie bar stresses that include the effects of all three components of nonlinear temperature distribution. Figure 3.15(a) also shows a rather rapid increase in tie bar stress as it nears the LCJ. The information in this figure illustrates that tie bar stresses predicted by SGDT are much lower than actual stresses, indicating that SGDT may not adequately assess stresses in tie bars and that including the other two components shown in Figure 3.1 should be considered for proper design of tie bars.

Figure 3.15(b) shows the transverse movement of the slab at the LCJ. It explains the mechanism of tie bar stress development at the LCJ when all three components are considered. The axial contraction causes frictional stress to develop at the interface between slab and subbase, which induces stresses in the tie bar. The concrete at the bottom of the slab will expand if there is no horizontal restraint. In real pavement, restrain exists at the LCJ due to the symmetry condition shown in Figure 3.5. Additional stress is produced when the expansion at the bottom is restrained. Figure 3.15(b) shows that the additional stress plays an important role in the development of stresses in tie bars.
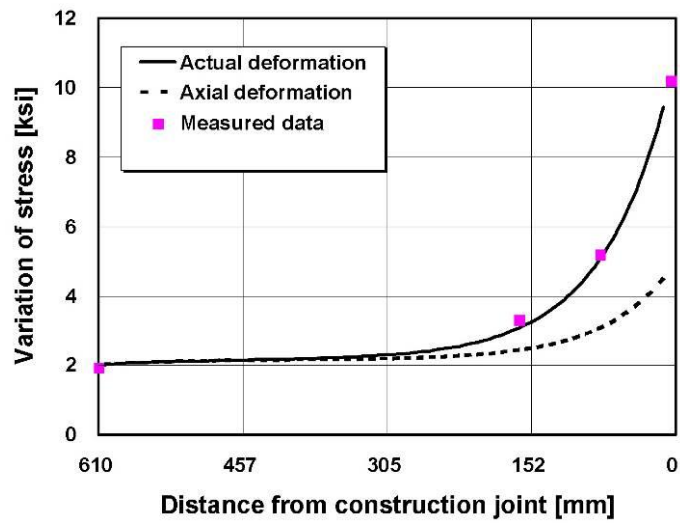
(a) Distribution of tie bar stress
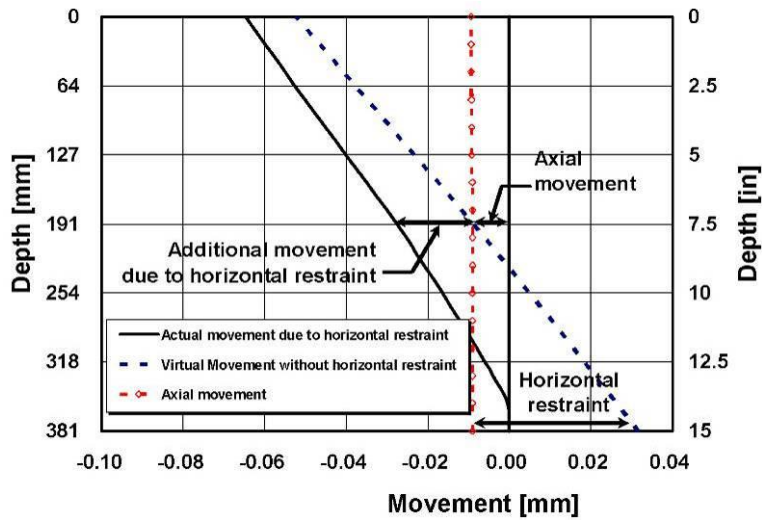


(b) Movement of concrete at construction joint in transverse direction

*Figure 3.15: Tie bar stress and movement at construction joint*

54

## 3.3 Summary

Tie bar design is currently based on SGDT. However, the following results obtained from field experimentation showed that SGDT is not adequate to accurately analyze the behavior of concrete pavements: (1) concrete temperatures evaluated at various depths from the concrete placement showed substantial variations through the slab depth; (2) concrete slab displacement measurements at the free edge exhibited daily curling behavior; and (3) quite different stresses occurred in tie bars placed at different depths. Accordingly, an improved numerical model was developed to analyze a concrete pavement with tie bars at LCJs. First, three-dimensional finite element model which uses three-dimensional solid elements in the mesh representation of concrete and tie bars was developed. However, modeling the tie bar with three-dimensional solid elements significantly increase the total number of finite elements. Three-dimensional analysis with a large number of solid elements is very time-consuming. Accordingly, a two-dimensional finite element model – a simplified model which uses plane strain elements for modeling concrete – was introduced. This simplified model is possible because CRCP is sufficiently long with repeated geometry and it is subjected to environmental loading only in this analysis – temperature gradients do not change along the longitudinal axis. To verify the validity of plane strain model, the results from numerical analysis were compared with field measurements – transverse displacements across the LCJ, concrete stresses, and tie bar stresses. The comparison indicated a good correlation between them when both frictional restraint and curling effects were included in the analysis. On the other hand, when only frictional resistance was included in the analysis, which is the case when SGDT is applied, there was a large discrepancy between measured and predicted values.

# CHAPTER 4. NUMERICAL PARAMETRIC STUDY ON TIE BAR DESIGN FACTORS

The influences of multiple lane ties and pavement geometries on the behavior of CRCP were analyzed through parametric studies using the plane strain finite element model introduced in Section 3.2.1. The evaluations were conducted for different numbers of lanes tied together, vertical locations of tie bars, pavement thicknesses, and tie bar spacings as shown in Table 4.1. As shown in Figure 4.1(a), four levels of pavement thickness were selected, and in case of 15 inch-thick pavements, two layers of tie bars were installed according to the TxDOT Design Standards for CRCP (TxDOT, 2003). As Figure 4.1(b) shows, with the exception of 15 inch-thick pavements, three levels of vertical location of tie bars were considered: above mid-depth, at mid-depth, and below mid-depth. The 15 inch-thick pavement was excluded because of two layer tie bar placement. The tie bar spacing was assumed in two ways: (1) constant as 3 ft and (2) varying as given in Table 4.2 according to the TxDOT Design Standards for CRCP (TxDOT, 2003). For each case in Table 4.1, the behavior of CRCP was evaluated for an incremental number of tied lanes from 2 to 10.

The diameter and length of tie bars were 0.75 and 50 in., respectively. The CTE, elastic modulus, and Poisson's ratio were $6 \times 10^{-6}$ /$^{\circ}$F, $6 \times 10^{6}$ psi, and 0.15 for concrete and $6.4 \times 10^{-6}$ /$^{\circ}$F , $2.9 \times 10^{7}$ psi, and 0.3 for tie bars, respectively. The modulus of subgrade reaction was 400 psi/in. in compression and zero in tension. The frictional stress-slip stiffness was 150 psi/in. with a yield-slip of 0.02 in. The bond stress-slip relationship was assumed as shown in Figure 3.8. Figure 4.1(c) describes the thermal loading applied to pavements, which is composed of a seasonal drop and a daily variation. A conservative seasonal drop of -68 $^{\circ}$F from summer to winter was assumed, referring to the annual variation of the average temperature of concrete pavements in Texas (Suh and Won, 2007). As for the daily variation, a nonlinear negative thermal gradient was assumed at -1.5 $^{\circ}$F per inch of slab thickness.

*Table 4.1: Analysis cases*

| Pavement Thickness (in.) | Vertical Location of Tie Bars and Tie Bar Spacing | | | | | |
|---|---|---|---|---|---|---|
| | Above Mid-Depth | | At Mid-Depth | | Below Mid-Depth | |
| | Constant | Varying | Constant | Varying | Constant | Varying |
| 8 | 8-U-C | 8-U-V | 8-M-C | 8-M-V | 8-L-C | 8-L-V |
| 10 | 10-U-C | 10-U-V | 10-M-C | 10-M-V | 10-L-C | 10-L-V |
| 12 | 12-U-C | 12-U-V | 12-M-C | 12-M-V | 12-L-C | 12-L-V |
| 15 | - | - | 15-M-C[a] | 15-M-V[a] | - | - |

[a] 'M' does not mean that tie bars are placed at mid-depth. Tie bars are placed in two layers as shown in Figure 4.1(a).

*Table 4.2: Variation of tie bar spacing (ft)*

| Pavement Thickness (in.) | Pavement Width (ft) | | | | | | | | |
|---|---|---|---|---|---|---|---|---|---|
| | 24 | 36 | 48 | 60 | 72 | 84 | 96 | 108 | 120 |
| 8 | 3 | 3 | 3 | 3 | 3 | 3 | 2.5 | 2.5 | 2 |
| 10 | 3 | 3 | 3 | 3 | 2.5 | 2.5 | 2 | 1.5 | 1.5 |
| 12 | 3 | 3 | 3 | 2.5 | 2 | 2 | 1.5 | 1.5 | 1 |
| 15 | 3 | 3 | 3 | 3 | 3 | 3 | 2.5 | 2.5 | 2 |
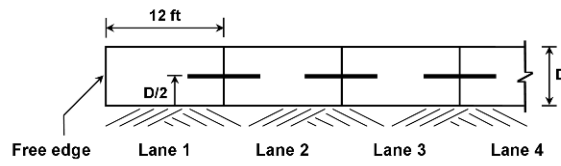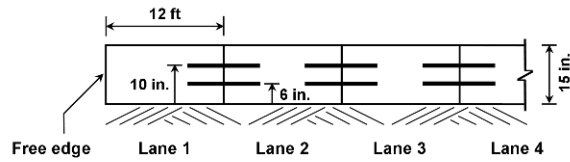


(a) Four levels of pavement thickness
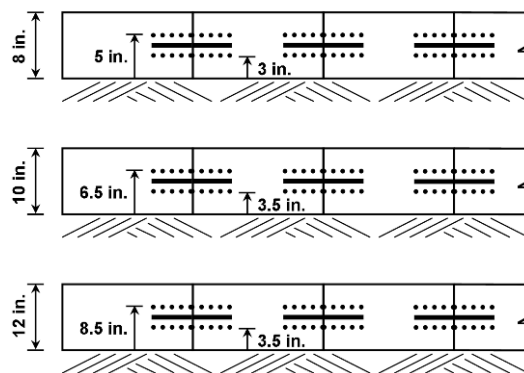


(b) Three levels of tie bar location
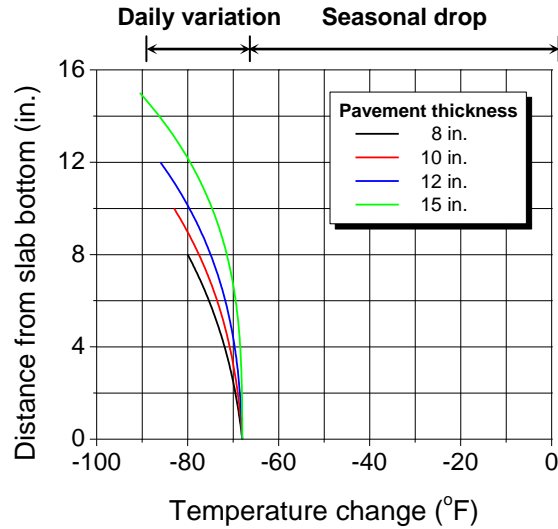
(c) Thermal loading

*Figure 4.1: Analysis descriptions and conditions*

## 4.1 Effect of Number of Lanes Tied Together

Case 12-M-C was analyzed by varying the number of tied lanes. Figure 4.2 shows that the surface deflection of each inside lane is quite similar to one another when many lanes are tied. The tie bar stress and the bond stress between tie bars and surrounding concrete are represented in Figure 4.3. In this figure, for clarity of presentation, the length of a whole tie bar, which is 50 in., is shown in a lane width. The tie bar stress increases rapidly as it gets closer to LCJs and each tie bar has its peak stress at its middle point (LCJs). Similar tendencies are found in the distribution of bond stress. Another fact worthy of note is that bond slip between tie bars and concrete occurs when many lanes are tied. The bond stress is constant as zero near the middle of the third to seventh tie bars in the ten-lane pavement. Bond slip between tie bars and concrete in multiple-lane pavements results in the tie bar stress having flat peaks as well as sharp peaks, and furthermore gives the flat peaks similar values. The range where the bond slip between tie bars and concrete occurs is identical to the range where the tie bar stress has flat peaks.

0-6190-1
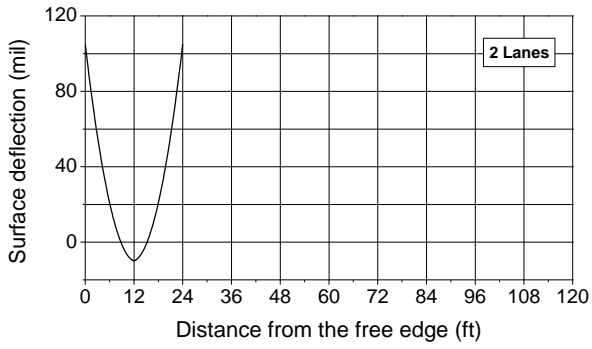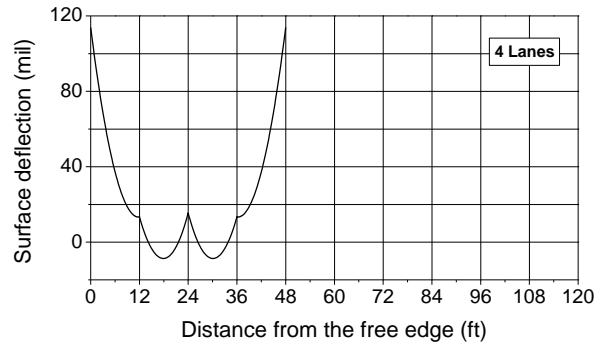
(a) Two-lane pavement

(b) Four-lane pavement
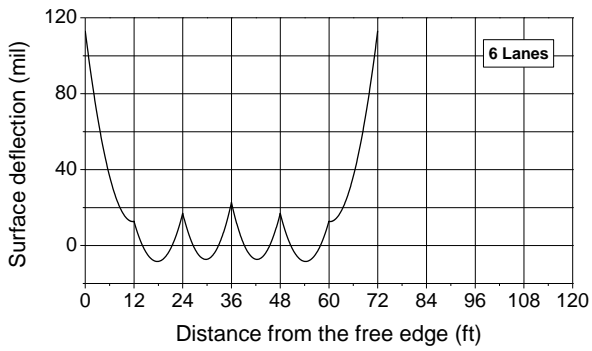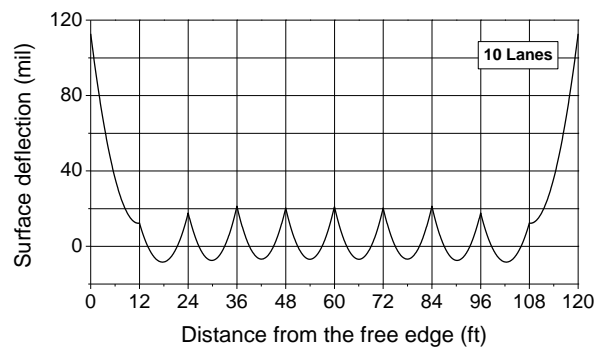
(c) Six-lane pavement

(d) Ten-lane pavement

*Figure 4.2: Surface deflection in Case 12-M-C*
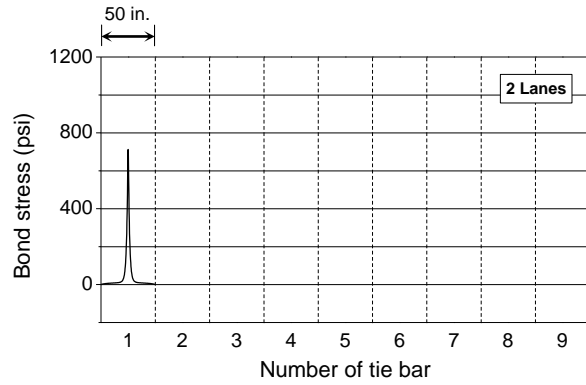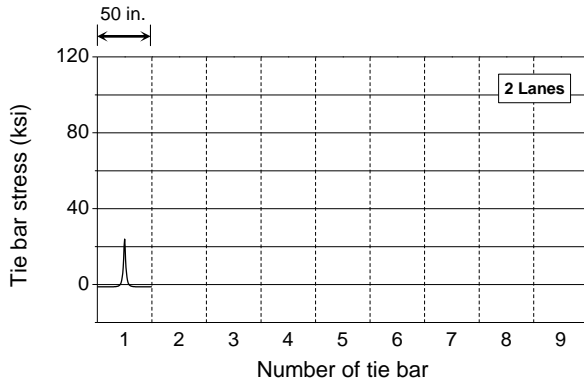
(a) Two-lane pavement
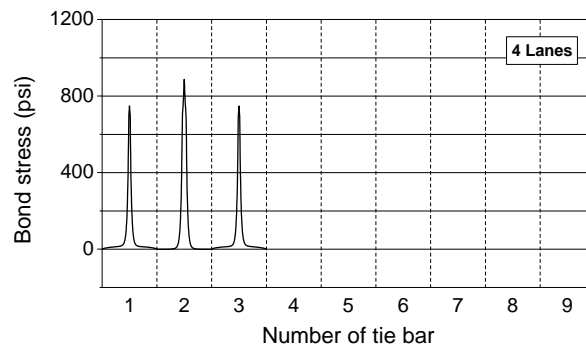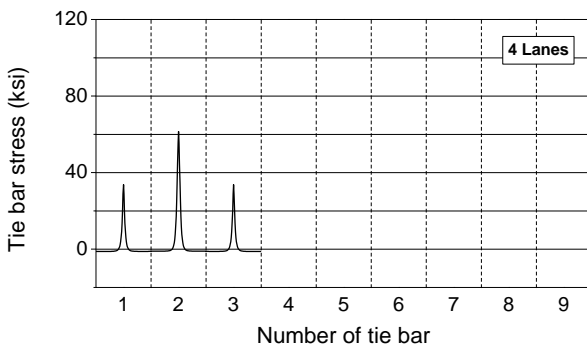


(b) Four-lane pavement
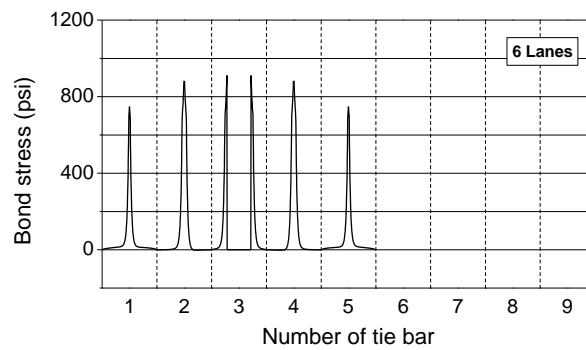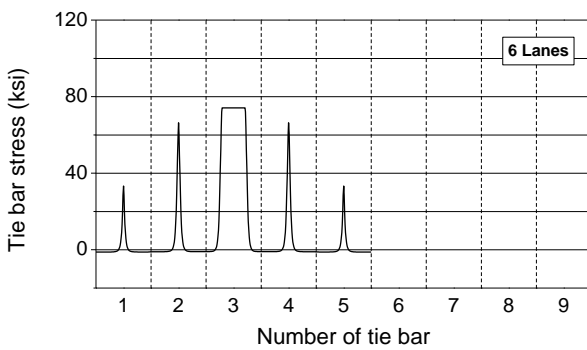


(c) Six-lane pavement

*Figure 4.3: Tie bar stress and bond stress in Case 12-M-C*
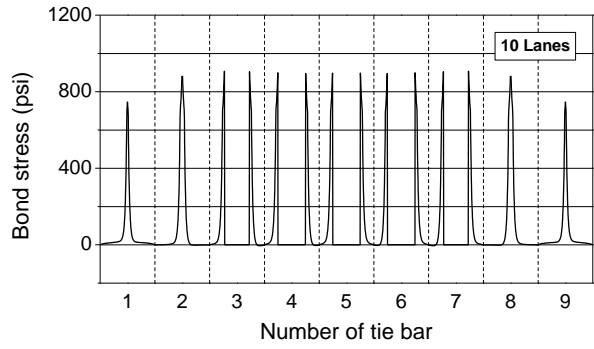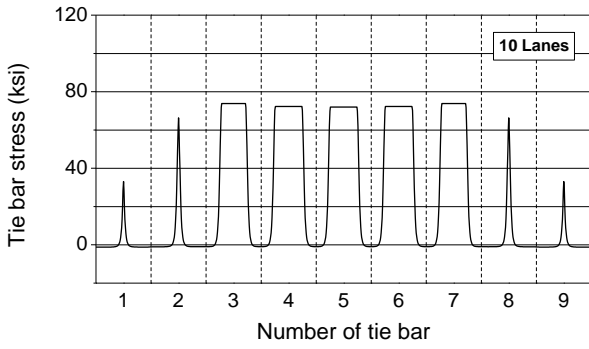
(d) Ten-lane pavement

*Figure 4.3: Tie bar stress and bond stress in Case 12-M-C (continued)*
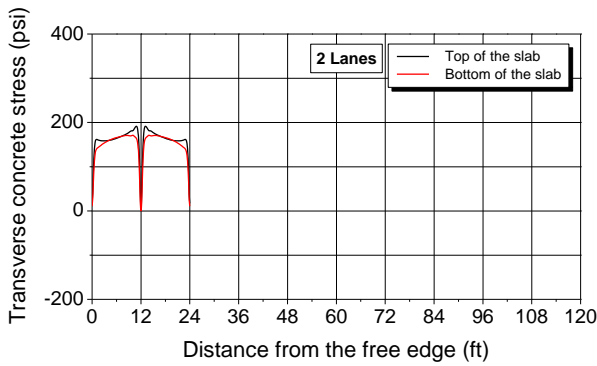


(a) Two-lane pavement
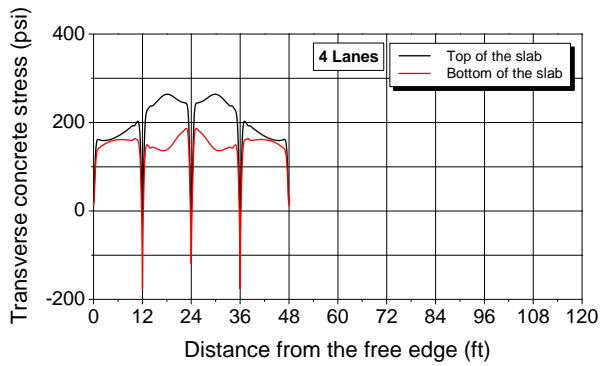


(b) Four-lane pavement
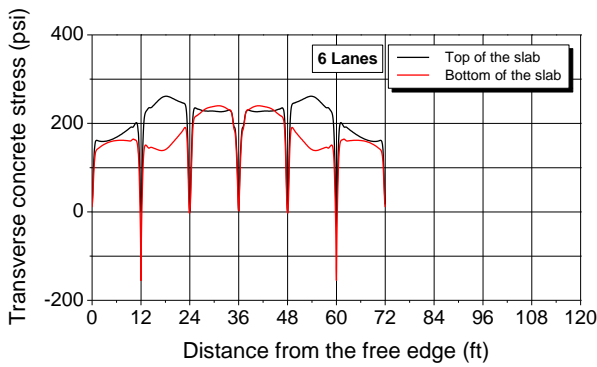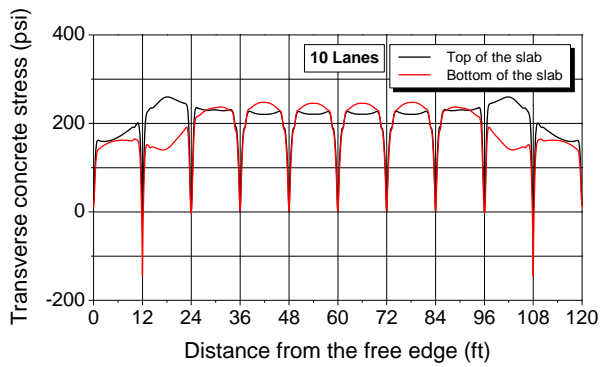


(c) Six-lane pavement



(d) Ten-lane pavement

*Figure 4.4: Transverse concrete stress along the top and bottom of the slab in Case 12-M-C*

62
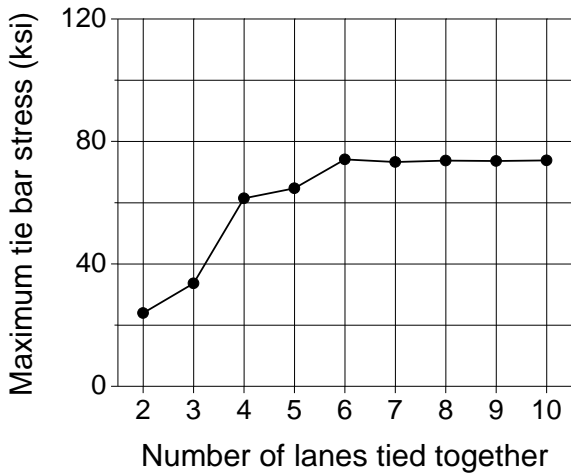
(a) Maximum tie bar stress
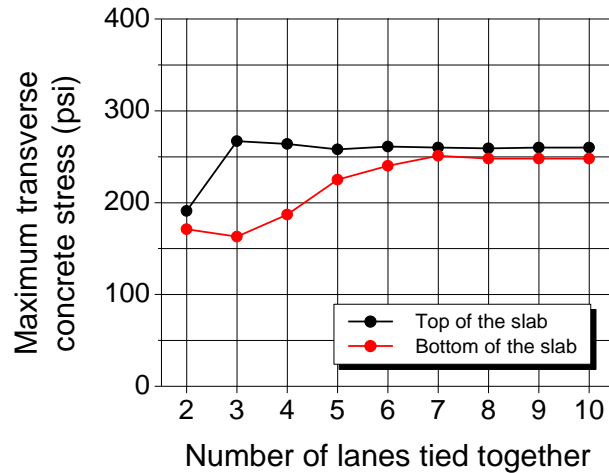
(b) Maximum transverse concrete stresses
at the top and bottom of the slab

*Figure 4.5: Maximum tie bar stress and concrete stress according to the number of tied lanes in Case 12-M-C*

Figure 4.4 shows the transverse concrete stresses along the top and bottom of the slab. Tensile concrete stress develops in general but the concrete stress decreases rapidly when approaching the LCJs; the bond resistance along a tie bar prevents a LCJ from separating if bond slip between tie bars and concrete does not occur, and therefore the two adjacent lanes restrain each other at the bottom of the LCJ when they bend upward due to thermal gradient. Maximum concrete stress at the top of the slab occurs in lane number 2 (if the outermost lane is denoted as lane number 1 and lane number increases as it moves towards inside lanes). Tie bars placed at both sides of the lane number 2 have lower probability of undergoing bond slip between tie bars and concrete so that they greatly restrain the thermal gradient-induced bending of the lane number 2. The maximum concrete stress at the bottom of the slab occurs in one of the inside lanes where tie bars in those lanes undergo bond slip between tie bars and concrete. The maximum concrete stress that occurs in lanes inside lane number 2 is similar in those lanes when many lanes are tied because bond slip between tie bars and concrete could occur along the tie bars placed between these lanes.

Figure 4.5 shows the maximum tie bar stresses and concrete stresses with respect to the number of tied lanes. The maximum tie bar stress and concrete stress at the bottom of the slab increase as more lanes are tied, but converge when six or more lanes are tied because some tie bars undergo bond slip between tie bars and concrete in these conditions. The maximum concrete stresses at the top of the slab are similar to one another except for the two-lane pavement because it occurs in lane number 2 regardless of the number of tied lanes. If the assumptions made in SGDT are true, the maximum tie bar stress should increase steadily with the number of tied lanes even if more than six lanes are tied.

0-6190-1
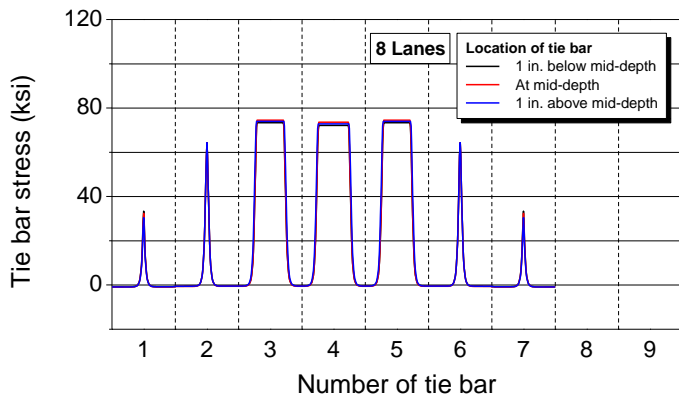
(a) Tie bar stress in eight-lane pavement
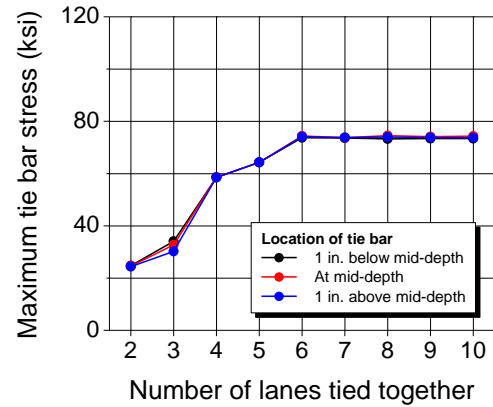
(b) Maximum tie bar stress
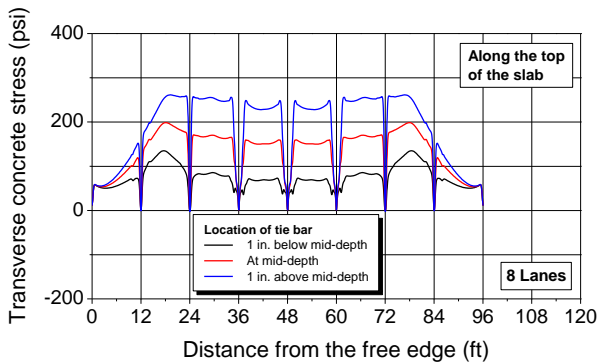
(c) Concrete stress along the top of the slab in eight-lane pavement
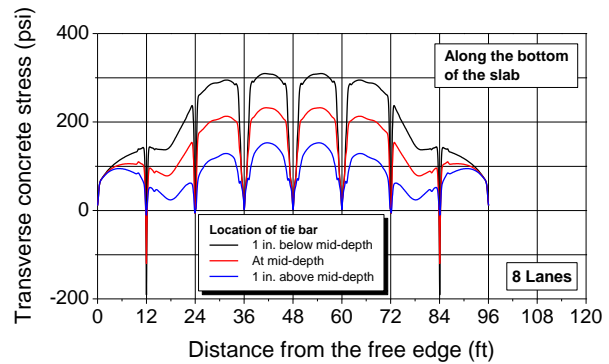
(d) Concrete stress along the bottom of the slab in eight-lane pavement
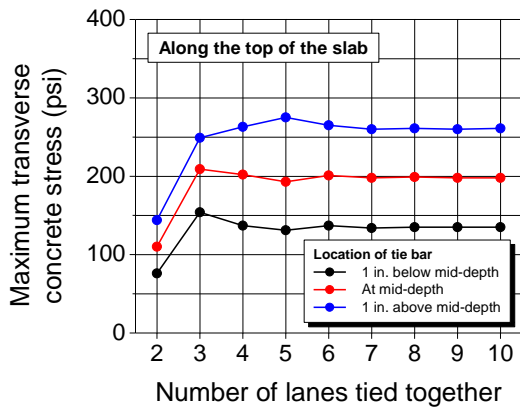
(e) Maximum concrete stress at the top of the slab
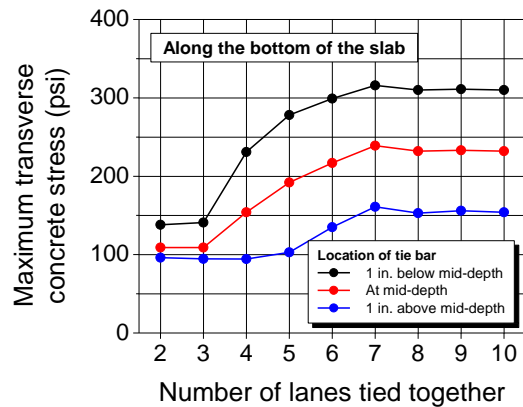
(f) Maximum concrete stress at the bottom of the slab

*Figure 4.6: Effect of vertical location of tie bars in 8 inch-thick pavements*

## 4.2 Effect of Vertical Location of Tie Bars

Cases 8-L-C, 8-M-C, and 8-U-C were analyzed by varying the number of tied lanes. Figure 4.6 shows the tie bar stress and concrete stresses. The tie bar stress is not significantly influenced by the vertical location of tie bars. This is likely because the seasonal temperature drop rather than the daily thermal gradient dominantly contributes to the development of tie bar stress. However, the vertical location of tie bars affects the concrete stress considerably. The restraint intensity exerted by a tie bar becomes greater as the tie bar is placed closer to the concrete surface. Similar results are obtained in cases of 10 and 12 inch-thick pavements where a relatively small change in the vertical location of tie bars results in a large difference in concrete stress, which can not be explained by SGDT. These results imply that the current practice of placing tie bars at mid-depth might be the proper way to reduce the longitudinal cracking.

## 4.3 Effect of Pavement Thickness

The concrete pavements with four different thicknesses were analyzed by varying the number of tied lanes: Cases 8-M-C, 10-M-C, 12-M-C, and 15-M-C. Figure 4.7 shows the tie bar stress and concrete stresses. In Case 15-M-C, the upper tie bars experience higher stress than the lower tie bars because of the negative nonlinear thermal gradient (see Figure 3.5). Furthermore, unlike the upper tie bar, the maximum stress in the lower tie bar increases steadily as more lanes are tied. This result can be understood that bond slip between tie bars and concrete does not occur along the lower tie bars even when many lanes are tied. The maximum tie bar stresses are smaller in Case 15-M-C than in the other cases due to two layer tie bar placement.

In Case 15-M-C, unlike the other cases, the maximum concrete stresses at the top and bottom of the slab occur in the middle lane and in the outermost lane, respectively. This is because the tie bars do not undergo bond slip between tie bars and concrete. The maximum concrete stress increases as the pavements get thicker; in other words, the temperature difference between the top and bottom of the slab increases. The maximum top stress increases by a large amount when the pavement thickness changes from 12 to 15 in. because the upper tie bars are placed 2.5 in. above the mid-depth in a 15 inch-thick slab (see Figure 4.1(a)). The maximum bottom stress in Case 15-M-C changes little up to six lanes because it occurs in the outermost lane regardless of the number of tied lanes. However, the maximum-occurring lane moves to the middle lane after seven lanes, so that the maximum bottom stress starts to increase with the number of tied lanes.

## 4.4 Effect of Tie Bar Spacing

TxDOT Design Standards for CRCP (TxDOT, 2003) require that tie bars be placed more closely as more lanes are tied. To investigate the effect of tie bar spacing, Cases 10-M-C and 10-M-V

65

were analyzed by varying the number of tied lanes. The numbers represented in Figure 4.8 indicate tie bar spacings in feet. The tie bar stress and the number of tie bars that undergo bond slip between tie bars and concrete increase with the tie bar spacing. The concrete stress increases as the tie bar spacing decreases because the restraint intensity exerted by tie bars becomes greater as tie bars are placed more closely. The pattern of the concrete stress curve is slightly different depending on the tie bar spacing. This is because the tie bar spacing influences the bond stresses along tie bars, and consequently affects the distribution of concrete stress. Similar results are also obtained for the pavements with different thicknesses.

0-6190-1
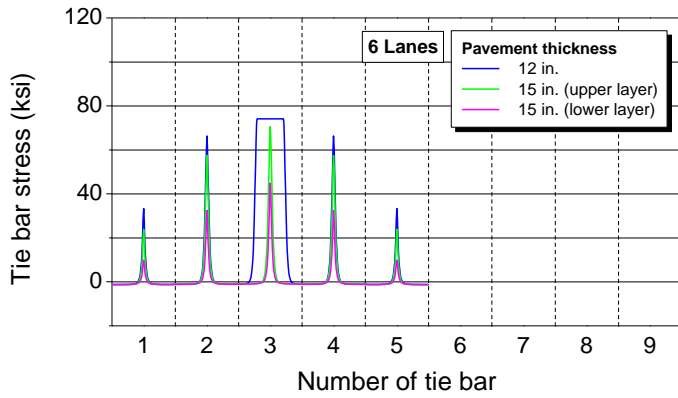
(a) Tie bar stress in six-lane pavement
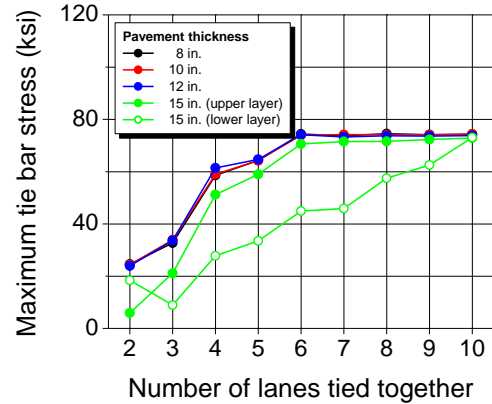
(b) Maximum tie bar stress
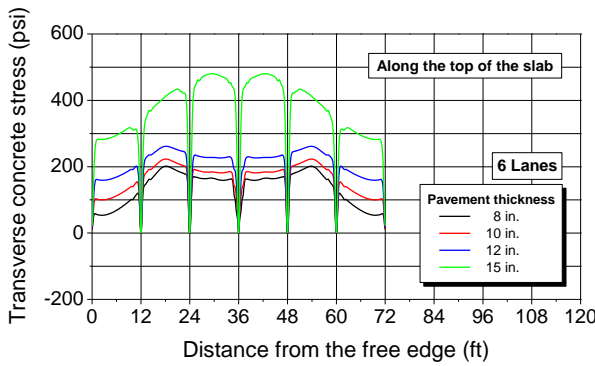
(c) Concrete stress along the top of the slab in six-lane pavement
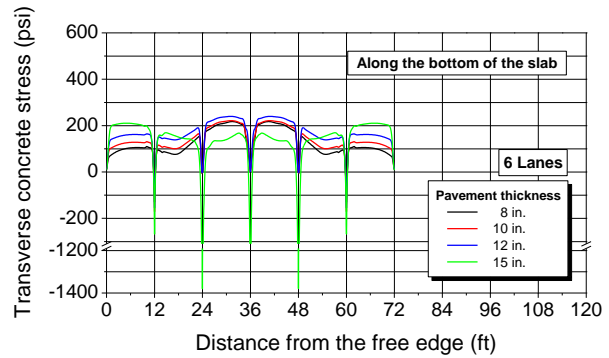
(d) Concrete stress along the bottom of the slab in six-lane pavement
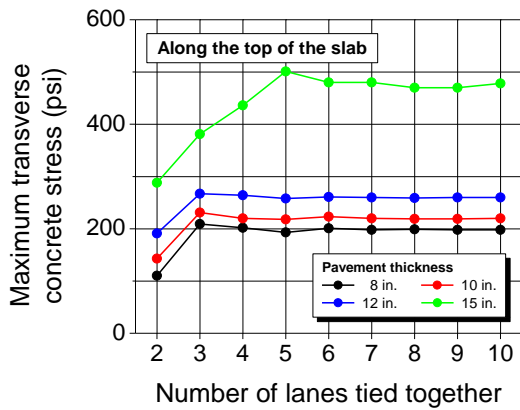
(e) Maximum concrete stress at the top of the slab
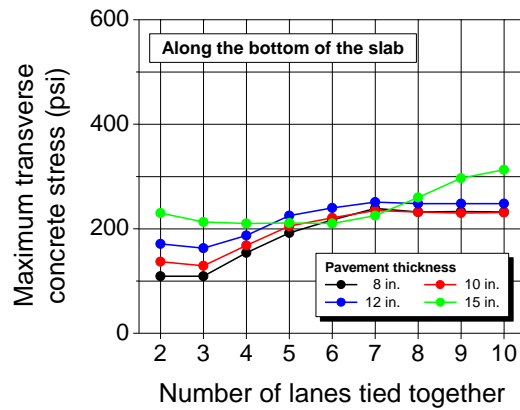
(f) Maximum concrete stress at the bottom of the slab

*Figure 4.7: Effect of pavement thickness*

67
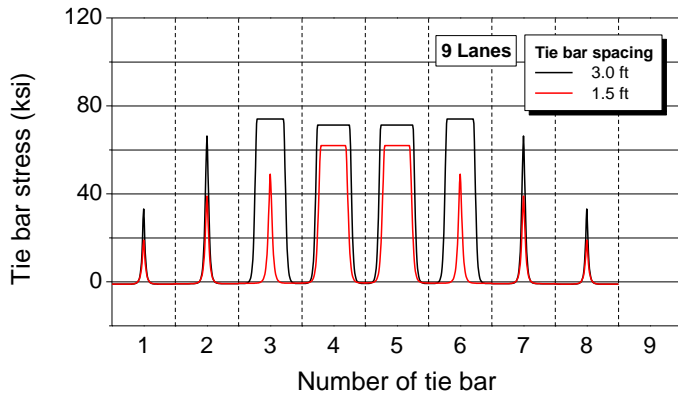
(a) Tie bar stress in nine-lane pavement
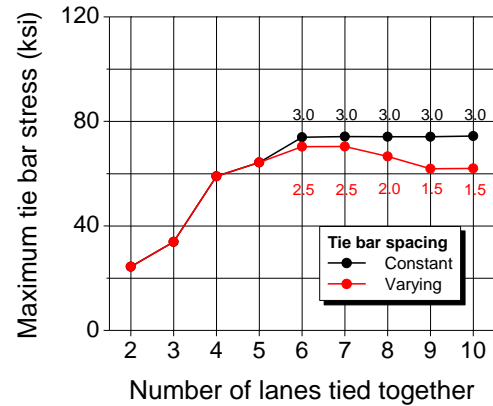
(b) Maximum tie bar stress
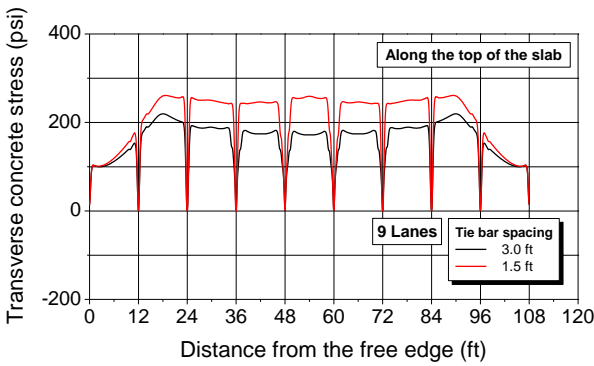
(c) Concrete stress along the top of the slab
in nine-lane pavement
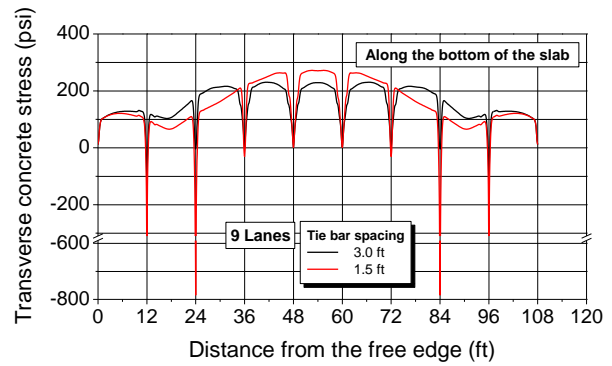
(d) Concrete stress along the bottom of the slab
in nine-lane pavement
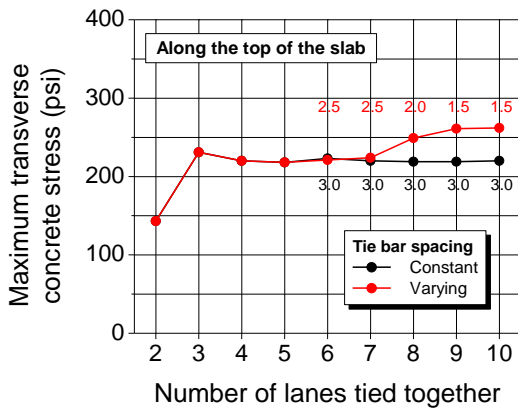
(e) Maximum concrete stress
at the top of the slab
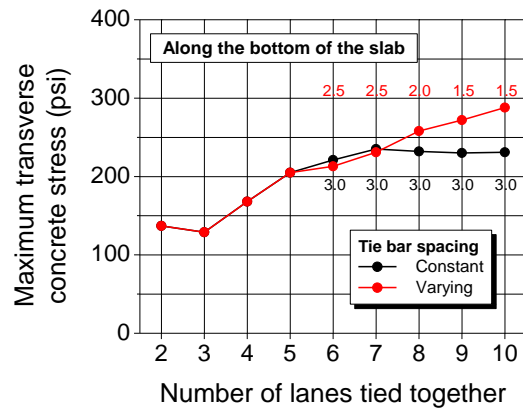
(f) Maximum concrete stress
at the bottom of the slab

*Figure 4.8: Effect of tie bar spacing in 10 inch-thick pavements*

0-6190-1

## 4.5 Effect of Use of Dowel Bars

To investigate the effect of dowel bar placement, the six-lane pavement in Case 12-M-V was analyzed with three different limits of the width of tied lanes: (1) no dowel bars; (2) dowel bars are placed every three lanes (two three-tied lanes); and (3) dowel bars are placed every two lanes (three two-tied lanes). It is assumed that the diameter of the dowel bar is 1.25 in. and that no bond resistance exists between dowel bars and surrounding concrete. The tie bar spacing is 2 ft in case of no dowel bars, and the tie bar and dowel bar spacings are 3 ft when dowel bars are used (see Table 4.2). Figure 4.9 shows the analytical results for the three different dowel bar arrangements. Each tied lane behaves similarly; when dowel bars are placed every two lanes, the numerical results of three two-tied lanes are similar to one another, and moreover they are similar to those of the two-lane pavement (see Figures 4.2(a), 4.3(a), and 4.4(a)). It can be inferred from this result that dowel bars make each tied lane behave independently.
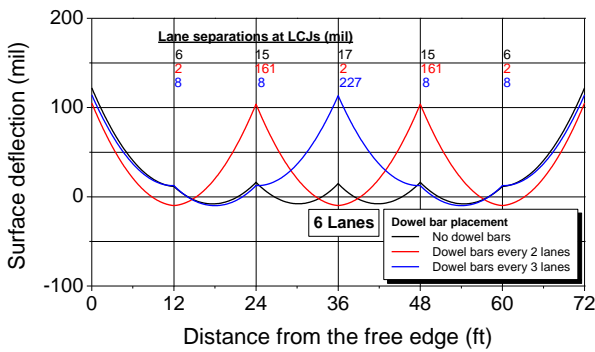


(a) Surface deflection and lane separation     (b) Tie bar stress
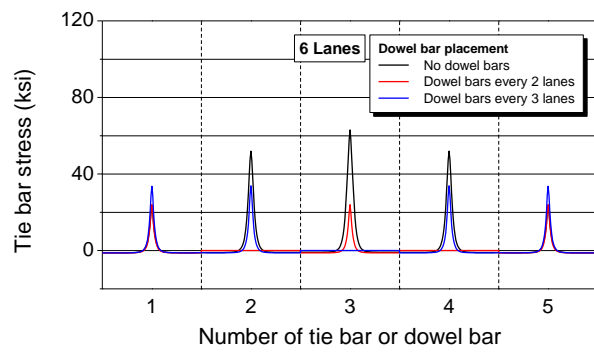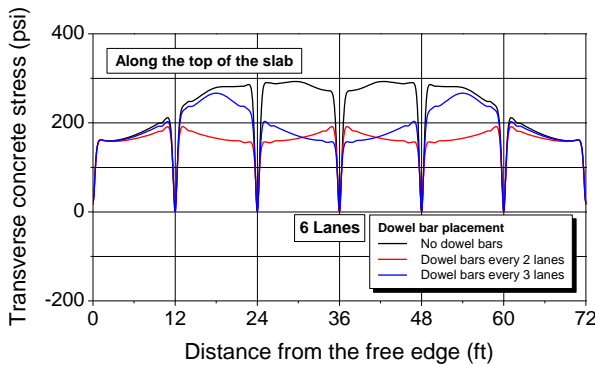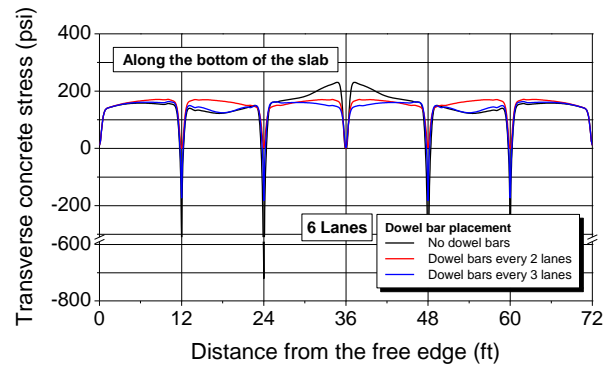
(c) Concrete stress along the top of the slab     (d) Concrete stress along the bottom of the slab

*Figure 4.9: Effect of dowel bar placement in six-lane pavement of Case 12-M-V*

69

0-6190-1
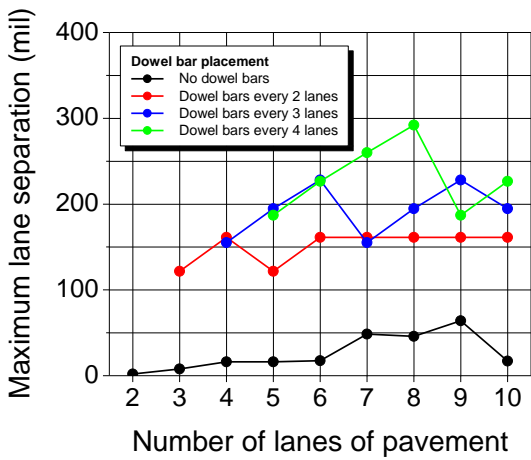
(a) Maximum lane separation
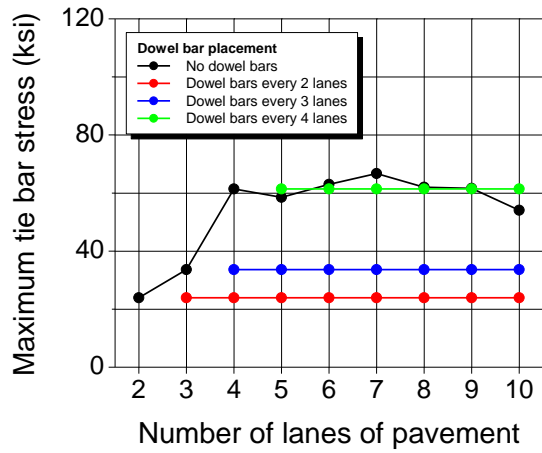


(b) Maximum tie bar stress
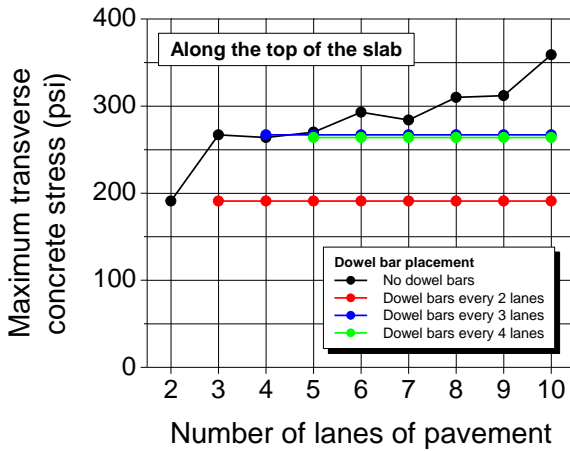


(c) Maximum concrete stress
at the top of the slab
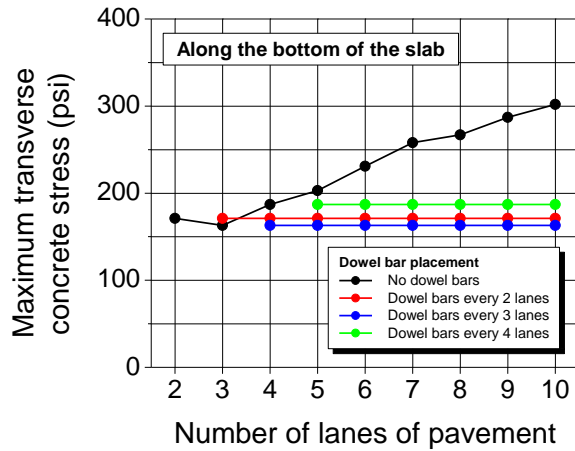


(d) Maximum concrete stress
at the bottom of the slab

*Figure 4.10: Effect of dowel bar placement in Case 12-M-V*

The same analyses are performed for the two- to ten-lane pavements in Case 12-M-V with four different maximum numbers of lanes that could be tied. The tie bar and dowel bar spacings are 3 ft when dowel bars are used while the tie bar spacing varies as given in Table 4.2 when no dowel bars are used. Figure 4.10 shows the analytical results for the four different dowel bar

70

0-6190-1

arrangements. As expected, the maximum tie bar stress decreases as more LCJs have dowel bars. However, placing dowel bars every four lanes seems to hardly reduce the maximum tie bar stress, compared with that of the case of no dowel bars. This is because the tie bar spacing is larger in the former case even though the maximum number of tied lanes is smaller. The maximum concrete stress also decreases generally as more LCJs have dowel bars and it decreases more in wider pavements. On the other hand, the maximum lane separation becomes much larger when dowel bars are used.

The reason why the lines in Figure 4.10(a) are not flat is that the maximum lane separation depends on the dowel bar arrangement. For example, when the maximum number of lanes that could be tied in a nine-lane pavement is four, the dowel bars can be arranged in five different ways: 4-tied lanes+4-tied lanes+1 lane, 4+3+2, 4+2+3, 4+1+4, and 3+4+2. Among these, the maximum lane separation has the smallest value when the pavement is composed of four-tied lanes, one lane, and four-tied lanes.

## 4.6 Effect of Wheel Loading

To examine the combined effect of traffic and environmental loading on concrete stresses, the four-lane pavement in Case 10-M-C was analyzed. As shown in Figure 4.11, a combined traffic loading, self-weight, and temperature gradient was applied to the concrete pavement. Considering the numerical model used in this analysis is two-dimensional, the magnitude of wheel loading was adjusted so that the surface deflection obtained by two-dimensional analysis is the same with that obtained by three-dimensional analysis. Accordingly, the wheel loading of 8 psi was used instead of a general value of 80 psi. The unit weight of concrete was assumed to be 145 $lb/ft^3$.
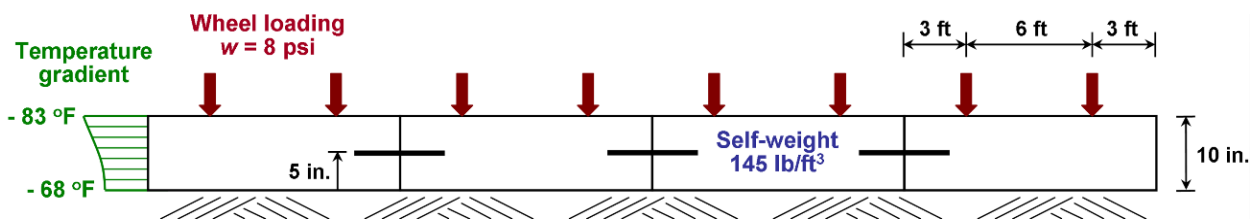


*Figure 4.11: Combined traffic loading, self-weight, and temperature gradient*

Figures 4.12(a) and 4.12(b) show the surface deflection and the transverse concrete stress along the top of the slab, respectively. As shown in Figure 4.12(a), the pavement curls up when temperature gradient is applied. The combined wheel loading and self-weight makes the curled-up pavement sink down on the whole. It is interesting that the combined wheel loading and self-weight causes larger additional surface deflections at the end of each lane than in the middle of each lane. This is because the combined wheel loading and self-weight is applied to the curled-

71

up pavement. For the same reason, as shown in Figure 4.12(b), the combined wheel loading and self-weight results in larger additional transverse concrete stress in the middle of each lane than at the end of each lane. The same analyses were performed for the two- to ten-lane pavements in Case 10-M-C. Figure 4.12(c) shows the maximum concrete stresses at the top of the slab with respect to the number of tied lanes. As shown in this figure, the combined wheel loading and self-weight increases the maximum transverse concrete stress regardless of the number of tied lanes. However, the combined wheel loading and self-weight does not change the tendency that the maximum stresses are similar to one another regardless of the number of tied lanes except for the two-lane pavement. This is likely because the wheel loading and self-weight have almost nothing to do with bond slip between tie bars and concrete.
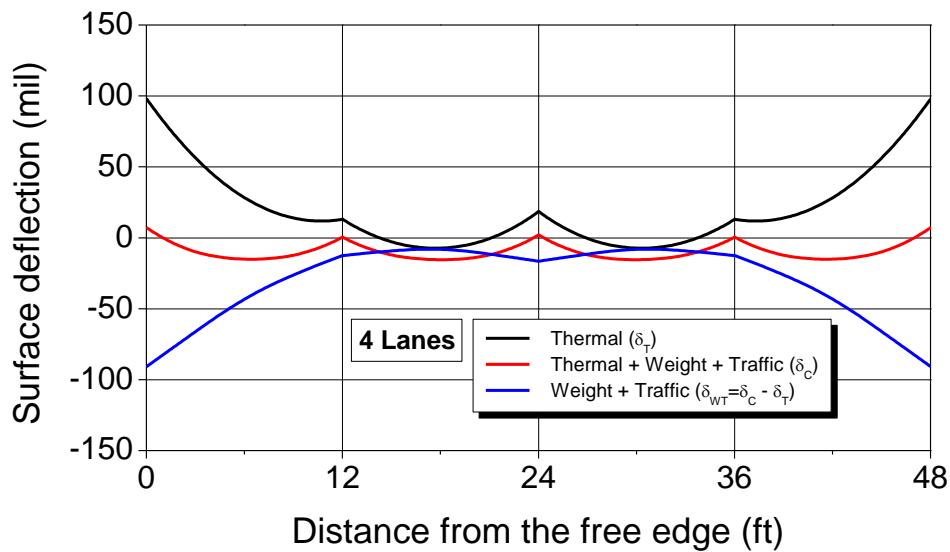


(a) Surface deflection in four-lane pavement

0-6190-1
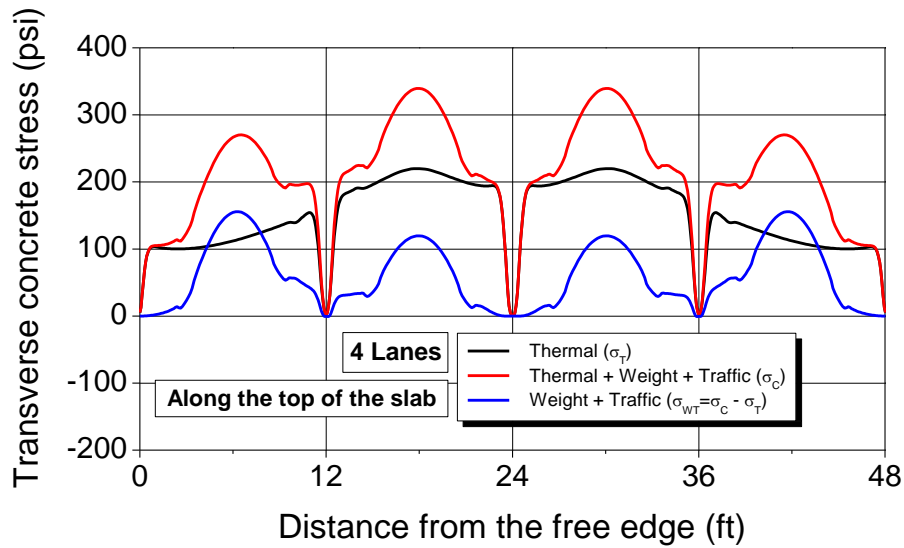
(b) Concrete stress along the top of the slab in four-lane pavement
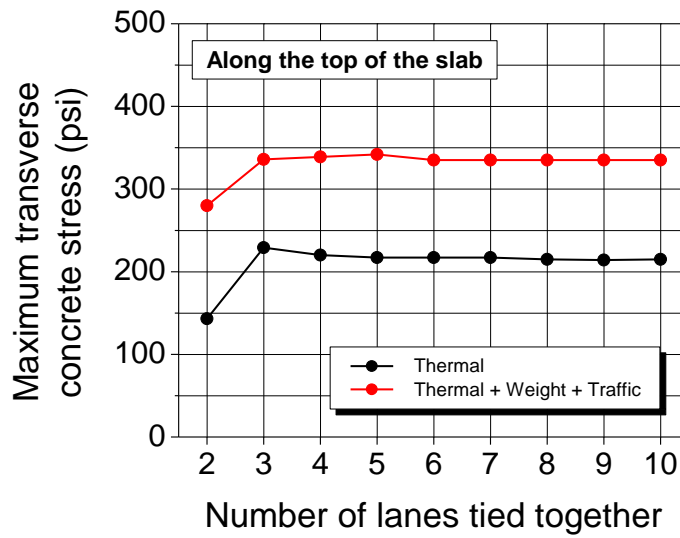


(c) Maximum concrete stress at the top of the slab

*Figure 4.12: Effect of wheel loading in 10 inch-thick pavements*

**4.7 Summary**

The effects of multiple lane ties and pavement geometries on the behavior of CRCP were investigated through parametric studies using the plane strain model. The evaluations were

73

0-6190-1

conducted for different pavement thicknesses, the vertical locations of tie bars, tie bar spacings, and the number of lanes tied together. The effectiveness of the use of dowel bars in LCJs was also evaluated through numerical analyses. The following conclusions, based on the numerical results, were reached: (1) the longitudinal cracking potential is greater in thicker concrete pavements; (2) tie bar depth has substantial effect on concrete stress; (3) the concrete stress at the top of the slab is much larger in two-layer tie bar placement than in one-layer tie bar placement; (4) higher tie bar stress and lower concrete stress develop as the tie bar spacing increases; (5) the maximum tie bar stress and concrete stress at the bottom of the slab increase as more lanes are tied but do not increase any more if bond slip between tie bars and concrete occurs due to tying many lanes; (6) the maximum concrete stresses at the top of the slab are similar to one another regardless of the number of tied lanes except for the two-lane pavement; (7) the use of dowel bars in LCJs makes each tied lane behave independently; and (8) the tie bar stress and concrete stress decrease as more LCJs have dowel bars, but the lane separation becomes much larger when dowel bars are used.

# CHAPTER 5 CONCLUSIONS AND RECOMMENDATIONS

The primary objective of this research project was to develop rational guidelines on the use of dowel bars in longitudinal construction joints (LCJs) – provide mechanically sound information on whether dowel bars are really needed at LCJs, and if they are, when and where they should be placed, and what the potential problems could arise. To thoroughly investigate concrete slab behaviors, detailed field testing was conducted. To achieve the primary objective of this study in a more effective way – developing guidelines for the use of dowel bars in LCJs solely based on the field testing data could require extensive field experimentations –, theoretical analysis was performed along with field experimentation. To evaluate the behavior of tied and/or doweled concrete pavements under environmental loading, field testing was conducted in several new CRCP construction projects in Texas, and the following conclusions were made:

(1) Concrete temperatures showed substantial variations through the slab depth. This variation causes slab curling and does not support the assumption made in SGDT, which is that there is no variation in temperature along the slab depth.

(2) Concrete slab displacement measurements at the free edge exhibited daily curling behavior. This behavior violates one of the assumptions made in SGDT, which is that the slab moves uniaxially in a transverse direction due to temperature variations.

(3) Quite different stresses occurred in tie bars placed at different depths. Much higher stresses were obtained in a tie bar placed close to the slab surface than in a tie bar placed at the mid-depth of the slab. This difference can be explained only if the curling effect is taken into account and not by SGDT.

(4) The opening of the LCJ at the early age resulted from mainly drying shrinkage of the concrete. Afterwards, the movement of the LCJ cycled in a large range stably, and was opposite to the changing trend of the air temperature. The movement of concrete at LCJ was larger than that in the longitudinal warping joint (LWJ).

(5) The concrete element was more restrained as it gets close to tie bars in the vertical direction. The movement of concrete at LCJ was larger in the doweled section than in the tied section, which means that tie bars provide more restraints on concrete elements.

(6) Transverse concrete stress was larger in the tied section than in the doweled section. It increased farther away from LCJ.

(7) Tie bar stresses increased rapidly as it gets close to the LCJ. Lower tie bar stresses developed as tie bars were placed more closely.

It was found from the field testing that SGDT is not adequate to accurately analyze the behavior of concrete pavements because of the assumptions of uniform temperature variations through the slab depth and a full contact between concrete slab and subbase. Accordingly, a more realistic

and improved numerical model was developed to analyze a concrete pavement with tie bars at LCJs. The model uses two-dimensional plane strain elements in the mesh representation of concrete and two-dimensional beam elements in the mesh representation of tie bars. To verify the validity of plane strain model, the numerical results were compared with the field data – transverse displacements across the LCJ, concrete stresses, and tie bar stresses. The comparison indicated a good correlation between them when both frictional restraint and curling effects were included in the analysis.

The influences of pavement geometries, multiple lane ties, and dowel bar placements at LCJs on the stresses in concrete and tie bars were analyzed through parametric studies using the numerical model. The evaluations were conducted for different pavement thicknesses, the vertical locations of tie bars, tie bar spacings, and the number of lanes tied together. The following conclusions, based on numerical results, were reached:

(1) Larger concrete stress occurs in thicker concrete pavements.

(2) The concrete stress at the top of the slab increases as the tie bar is placed closer to the concrete surface. In addition, it is larger in two-layer tie bar placement than in one-layer tie bar placement.

(3) Higher tie bar stress and lower concrete stress develop as the tie bar spacing increases.

(4) The maximum tie bar stress and concrete stress at the bottom of the slab increase as more lanes are tied but do not increase any more if bond slip occurs at the interface between steel and concrete due to tying many lanes. The maximum concrete stresses at the top of the slab are similar to one another regardless of the number of tied lanes except for the two-lane pavement.

(5) The use of dowel bars in LCJs makes each tied lane behave independently. The tie bar stress and concrete stress decrease as more LCJs have dowel bars, but the lane separation becomes much larger when dowel bars are used.

Although the stresses in tie bars and concrete increase as more lanes are tied together, the growth slows due to bond slip at the interface between tie bars and concrete. This means that the dowel bar placement instead of tie bars could reduce concrete stresses if it applies to wide pavements, while it could result in lane separation problems. On the other hand, concrete stresses do not increase any further if four or more lanes are tied together, and concrete stresses may not be high enough to cause longitudinal cracking. There are many miles of CRCP in Texas where more than four lanes and inside and outside concrete shoulders are tied together, with no longitudinal cracking. Accordingly, it is recommended from the findings in this study not to use dowel LCJs as is the current practice. It is also recommended to place tie bars at mid-depth as is the current practice.

# REFERENCES

Bažant, Z. P. Mathematical Modeling of Creep and Shrinkage of Concrete. John Wiley and Sons, Chichester, 1988.

Comité Euro-International du Béton. *CEB-FIP Model Code 1990: Design Code*, Thomas Telford, London, 1993.

*Continuously Reinforced Concrete Pavements, One Layer Steel Bar Placement*. TxDOT, September 2003. ftp://ftp.dot.state.tx.us/pub/txdot-info/cmd/cserve/standard/roadway/crcp 103.pdf. Accessed July 31, 2010.

*Continuously Reinforced Concrete Pavements, Two Layer Steel Bar Placement*. TxDOT, September 2003. ftp://ftp.dot.state.tx.us/pub/txdot-info/cmd/cserve/standard/roadway/crcp 203.pdf. Accessed July 31, 2010.

*DIANA 8.1.2 User's Manual*. TNO Building Construction, the Netherlands, 2003.

Ghali, A., R. Favre, and M. Eldbadry. *Concrete Structures: Stresses and Deformation*. Spon Press, New York, 2002.

Huang, Y. H. *Pavement Design and Analysis*. Pearson Education, Inc., Upper Saddle River, N.J., 2004.

Kawaguchi, T., and S. Nakane. Investigation on Determining Thermal Stress in Massive Concrete Structures. *ACI Materials Journal*, Vol. 93, No. 1, 1996, pp. 96-101.

Kim, D.-H., and M. Won. *Pilot Implementation of Optimized Aggregate Gradation for Concrete Paving*. Research Report 9026-01-1, Center for Transportation Research, University of Texas at Austin, 2008.

Kim, S.-M., M. C. Won, and B. F. McCullough. *Development of a Finite Element Program for Continuously Reinforced Concrete Pavements*. Research Report 1758-S, Center for Transportation Research, University of Texas at Austin, 1997.

Kim, S.-M., M. C. Won, and B. F. McCullough. *Three-Dimensional Nonlinear Finite Element Analysis of Continuously Reinforced Concrete Pavements*. Research Report 1831-1, Center for Transportation Research, University of Texas at Austin, 2000.

McCullough, B. F., and R. O. Rasmussen. *Fast Track Paving: Concrete Temperature Control and Traffic Opening Criteria for Bonded Concrete Overlays*. Task G, Final Report, FHWA, US Department of Transportation, 1998.

Mohamed, A. R., and W. Hansen. Effect of Nonlinear Temperature Gradient on Curling Stress in Concrete Pavements. In *Transportation Research Record: Journal of the Transportation Research Board*, No. 1568, Transportation Research Board of the National Academies, Washington, D.C., 1997, pp. 65-71.

Nam, J.-H., D.-H. Kim, S. Choi, and M. C. Won. Variation of Crack Width over Time in Continuously Reinforced Concrete Pavement. In *Transportation Research Record: Journal of the Transportation Research Board*, No. 2037, Transportation Research Board of the National Academies, Washington, D.C., 2007, pp. 3-11.

Suh, C. and M. Won. *Design Standards for CRCP for Each Texas Environmental Region*. CD-

ROM. Research Presentation 1700-P14, Center for Transportation Research, University of Texas at Austin, 2007.

Yu, H. T., L. Khazanovich, M. I. Darter, and A. Ardani. Analysis of Concrete Pavement Response to Temperature and Wheel Loads Measured from Instrumented Slabs. In *Transportation Research Record: Journal of the Transportation Research Board*, No. 1639, Transportation Research Board of the National Academies, Washington, D.C., 1998, pp. 94-101.

0-6190-1

# APPENDIX A

## GUIDELINES FOR THE CONSTRUCTION PRACTICES TO MINIMIZE LONGITUDINAL CRACKING

Since the latest TxDOT Design Standards for CRCP require a constant spacing for transverse steel or tie bars, regardless of how many lanes are tied together, the use of excessive transverse steel due to tying too many lanes together is not an issue anymore. The only issue would be whether there will be a higher potential for longitudinal cracking.

In general, dowels would not be needed at longitudinal construction joints (LCJs) for the purpose of reducing the risk of potential longitudinal cracking. There are many miles of CRCP in Texas where more than four lanes and inside and outside concrete shoulders are tied together, with no longitudinal cracking. On the other hand, longitudinal cracking is occasionally observed even where only two lanes with inside and outside concrete shoulders are tied together. Field investigations reveal that most of the longitudinal cracking problems in Texas are due to deficient saw-cut depth that does not meet TxDOT requirement, which is minimum of one-third slab thickness. To minimize the potential for longitudinal cracking, the following practices are recommended.

1) Good jointing practice
2) Quality concrete curing
3) Placement of tie bars within depth tolerances

1. Good jointing practice

   Most of the longitudinal cracks in Texas are due to poor jointing practice – too shallow saw-cut depth and/or late saw-cut. When hard coarse aggregates are used in concrete, joint saw-cut takes more time and is costly, which increases the chances of shallow saw-cut. Good jointing practice itself, in accordance with the requirements in Item 360 and paving standards, will reduce the potential for longitudinal cracking substantially.

2. Quality concrete curing

   Good quality concrete curing will reduce built-in curling in concrete, which reduces transverse concrete stress. It will also make concrete near the surface more impermeable and reduce concrete volume changes and stresses due to wetting and drying of concrete surface. The reduced concrete stresses will minimize the potential for longitudinal cracking.

3. Placement of tie bars within depth tolerances

   Tie bar stresses and transverse concrete stresses increase as tie bars are placed closer to

the concrete surface, increasing the potential for longitudinal cracking. The effect of the depth of tie bars is substantial, and tie bars should be always placed within depth tolerances.